

UNIVERSITY OF SOUTHAMPTON



DEPARTMENT OF SHIP SCIENCE

FACULTY OF ENGINEERING
AND APPLIED SCIENCE

LFE STABILISATION REPORT OF PRELIMINARY TRIAL

by

P.A. Wilson and A. Tang

Ship Science Report No. 57

November 1992

UNIVERSITY OF SOUTHAMPTON



DEPARTMENT OF SHIP SCIENCE

FACULTY OF ENGINEERING
AND APPLIED SCIENCE

LFE STABILISATION REPORT OF PRELIMINARY TRIAL

by

P.A. Wilson and A. Tang

Ship Science Report No. 57

November 1992

This report comprises of two parts. Part I is a study on the use of filters to improve rudder LFE stabilisation, which is an extension of the last report. Part II is divided into three main sections. Section A is concerned with the forced roll/LFE trials conducted in June onboard HMS Lancaster. Section B gives an up-date of the electronics hardware for the LFE signal conditioning unit. In section C, the test plan for the equipment with the CCU at Sultan is described.

PART I

Introduction

In Tang[4], it was found that the relative sharp rise in the high frequency response of the rudder in the rudder L.F.E. stabilisation (RLS) system has made it rather ineffective. An obvious way to improve the system performance would be to eliminate the high frequency content in the L.F.E. feedback signal, which does little to counteract the dominant motion response near the roll natural frequency. In theory, a low-pass filter can be used to eliminate the undesirable high frequency content. However, owing to the phase-lag characteristics of this type of filter, there are practical limitations. This has been pointed out by Baitis [1] and Van Amerongen [5] when low-pass filters were used for the RRS system. This phase-lag effect has been overlooked in Schmitke[3] when filtering was used in their numerical model based on strip theory. The resulting performance study of RRS, which has shown very favourable trends, should be taken with caution.

The present study is to incorporate some simple but realistic filters into the numerical model in order to examine their effects on the motion responses. It is anticipated that the phase-lag characteristics of low-pass filters would cause undesirable motion responses. Therefore, some phase-lead compensation circuits have been explored and applied in a cascade fashion in the system with the expectation that this will counter-balance the undesirable phase-lag incurred by the low-pass filters selected in this study.

This study is divided into three sections. In section one, a brief introduction of the filters used in this study and their transfer function characteristics is given. The effects of low-pass filter on motion responses are examined in some details in section two. Section three examines the effects of phase-lead compensation on the overall motion responses with RLS.

Basic Background

Filters are often used to emphasize or eliminate the frequency components of an electrical signal, such that a desirable signal is obtained. They are normally classified as low-pass, high-pass, band-pass and stop-pass, depending on the ranges of frequencies that are being suppressed. In this section, attention will be focused on some low-pass filters, looking at their basic characteristics and examining the transfer functions that govern the output to the input. In terms of hard-ware, these filters can be constructed using resistors, capacitors and operational amplifiers as the basic components.

A low-pass filter is one in which the pass band extends from zero frequency ($\omega = 0$) to a cut-off frequency ($\omega = \omega_c$). Ideally, a low-pass filter would pass signals from zero frequency up to the cut-off frequency with no amplitude attenuation and rejects all signals above ω_c , as illustrated in fig.1a, where ω_c is at 1.0 rad/sec. However, in practice, this ideal filter cannot be realised. The basic features of a low-pass filter can be demonstrated using a linear low-pass filter having a transfer function defined by:

$$T(j\omega) = \frac{1}{s\tau_f + 1}$$

where $s = j\omega$ and τ_f is the time constant, which has a single pole on the left hand real-axis of the complex-plane. Varying the excitation frequency from zero to a high value, the frequency response of the filter can be constructed. The resulting amplitude and phase response of this filter are given in fig. 2a and 2b. As can be seen from these figures, the amplitude response is far from the ideal and that the phase-lag is quite noticeable. Also, the cut-off frequency is not so readily recognized as in the ideal case. In practice, the cut-off frequency is defined as the frequency at which the amplitude response is 0.707, the half power point. In this particular case, it corresponds to 1 rad/s. This shows that the transition from the pass-band to the stop-band is rather slow and that undesirable frequency contexts are not suppressed totally. The attenuation of this filter in the transition band is in fact -6dB/octave. This transition band can be reduced to bring about a higher attenuation. For example, a second order filter with two poles on the left hand side of the complex plane can be used to achieve a -12db/octave attenuation. However,

a Butterworth filter is of more practical interest.

A Butterworth filter is defined by the transfer function below:

$$| T_n(j\omega) | = \frac{1}{(1 + \omega^{2n})^{1/2}}$$

By increasing the index n , the number of pole terms in the complex plane increases, which can bring the resulting amplitude response close to the ideal filter. For example, when $n=5$, the amplitude and phase responses are given in fig.3a and 3b. From these figures, it is quite clear that in order to suppress the unwanted frequency totally, the cut-off frequency should be at most about a third of that particular frequency. Within this pass-band, the phase-lag can be up to 100 degrees. Although the amplitude response can be 'improved' by increasing n , for example, for $n=5$ attenuation is about -30db/octave comparing with -60db/octave for $n=10$, the phase-lag incurred will also increase quite markedly (about twice the $n=5$).

Other types of filter such as the Chebyshev and Elliptic filter can also be used to reduce the transition band further. However, ripples are present in the amplitude response of these filters and the phase-lags are also higher than the Butterworth filters of the same order. Therefore, for the present study, only the linear filter and the Butterworth filter with $n=5$ will be used to explore their effects on the motion response.

Effects of Low-pass filters

For this part of the study, the RRS strategy with simple rate feedback has been used to examine the effects of the two low-pass filters in the last section. These filters, which are defined by their transfer functions, have been incorporated into the numerical ship motion model, suppressing the high frequency content of the feedback demand signal. A comparison of the r.m.s. roll motion response due to these filters are given in fig.4.a with the corresponding r.m.s. rudder rate demand in fig.4.b. The simulations were based on an ITTC two-parameter spectrum (long-crested) with a modal period of

12.4 seconds and a significant wave height of 5.5m. The cut-off frequency of the filters was set at 1 rad/s whilst the natural frequency of the vessel is about 0.42 rad/s.

From fig.4.a, it can be seen that the linear filter has improved the roll motion at quartering seas slightly whilst there is a marginal increase in the motion at other wave angles compared to the case of simple rate feedback. The corresponding rudder rate demand in fig.4.b suggests that if the feedback gain was increased, the overall motion response could be improved a bit further. The reduction in the rudder rate is due to the relatively wide transition band in the filter amplitude response with a gradual increase in attenuation, which effectively reduces the pre-set feedback gain. The relatively low phase-lag characteristic in the frequency range of interest and the fairly wide transition range have contributed little towards a more favourable motion response nor brought about any detrimental effects.

The resulting motion response with the application of the Butterworth filter is of more interest. In fig.4.a, it is quite apparent that between quartering to head seas regions, the resulting roll motions have been reduced more substantially, but on the other hand, for wave angles greater than 60 degrees, roll motions have in fact increased. The rudder rate in fig.4.b shows a similar trend. It is quite evident that some form of detuning process was brought about by the Butterworth filter. In order to find out what is causing this detuning effect, the process should be looked at in terms of the encounter frequency and not the wave-angles. Also, the phase relationships between the ship motions, wave moments and the stabiliser moments should be examined.

Diagrams 1a to 1c illustrate the phase relationships of a stabilised ship with simple rate feedback, which were drawn based on the response spectrum data. At low frequency, the roll motion leads the waves by about 90 degrees; near resonance, the phase difference is near zero, and at high frequency, the motion lags the wave by about 90 degrees. It can be said that at low and at high frequency, the wave moments and roll motions are about 90 degrees out of phase, and the induced motions are small, whilst near resonance, the phase angle is small and the induced motion is high. Therefore, the motion can be related to the cosine of the phase angle between the roll motion and the waves, i.e. if the stabiliser moment (S) brings the phase angle between the resultant wave moment ($W + S$) and motion (M) towards 90 degrees, the net effect is stabilisation, whilst if the

phase angle is moving towards zero degrees, then it is destabilisation.

It is quite clear that, at low frequency, the rate feedback is destabilising as illustrated in diagram 1.a. Near resonance, the rate feedback is very effective as it brings the phase difference between the wave moments and motion towards 90 degrees, whilst at high frequency, the stabilising effect is marginal due to the small stabilising moment available. Therefore, simple rate feedback is only effective when applied near resonance as was pointed out by Conolly [2].

Now, by introducing a Butterworth filter, the phase relationship between the stabiliser moments and the motions is altered. These phasor diagrams are illustrated in diagrams 2.a-2.c. At low frequency and at high frequency, the filter has brought about hardly any changes in the motion response. However, near the resonance region, the phase-lag affected by the filter has caused unfavourable phase relationships between the resultant wave moments and the motions, i.e. reducing the phase angle between the motion and the wave moments towards zero.

Having found what is causing the motion amplification, the trend in fig.4.a for the Butterworth filter can be explained more fully. In the quartering to head sea region (less than about 45 degrees), the encounter frequencies are about half the cut-off frequency. Although the near resonance response is destabilising, the sum total of the stabilising effects at the low frequency end has improved the overall motion response. However at 60 degrees, quite substantial part of the encounter frequency is near and slightly above the resonance frequency, which makes the phase-lag effect more prominent, with the resulting detuning effect augmenting the motion. At larger wave angles, i.e. higher frequency of encounter, the phase-lag effect at these frequency is marginal, but the response near resonance is still dominant. Hence there is an overall motion amplification. The same is true of the linear filter, except that the phase-lag effect is less obvious due the more gradual transition band.

The detuning effect of this Butterworth ($n=5$) low pass filter is even more noticeable when the cut-off frequency is placed near the natural roll frequency. In fig. 5a, it can be seen that the phase-lag introduced by the filter with a low-cut off frequency would amplify the motion by almost a factor of two compared to the high cut-off

frequency case. The rudder is in fact working harder in this case as shown by the higher rudder rate amplitudes in fig.5b. Unfortunately, it is not counteracting the motion effectively.

Phase-lead compensation

Hence, in the work presented thus far, the limitation of low-pass filters reported in Baitis [1] and Van Amerogen [5] for RRS is confirmed. Similar effects were also found when low-pass filters were applied to RLS.

To counteract the unfavourable phase-lag incurred by low-pass filters, phase lead compensation filters can be used. Typical responses of such a filter is shown in fig.6a and 6b, which is defined by the transfer function:

$$T(j\omega) = \frac{s\tau_f + a}{s\tau_f + b} \quad 0 \leq a \leq b$$

However, for the present study, the relatively low phase lead and the relatively high amplitude attenuation would make this filter rather ineffective. Instead, an all-pass filter will be used. This can be achieved by making $a=-1$ and $b=1$, giving a transfer function:

$$T(j\omega) = \frac{s\tau_f - 1}{s\tau_f + 1}$$

The amplitude and phase response are shown in fig.7a and 7b.

From an preliminary work, it was found that applying this all-pass filter to RRS with low-pass filter did not produce significant improvements. At close examination, it was apparent that this seemingly low performance stemmed from the fact that the improvement could only be small as the high frequency content in the roll feedback signal was quite low in the first place.

The all-pass filter was applied to the RLS case with Butterworth low-pass filter with the expectation of an increase in effectiveness of RLS. Unlike the RRS case in the

last section, the resulting phase relationship between the motions, moments and the rudder are difficult to follow because of the complex phasing between RLS, sway, roll and yaw. This means that it would be easier to find out how the phase-lead compensator affects the motion by varying the amount of phase-lead until the lowest r.m.s. motions are obtained. The amount of phase-lead can be adjusted by changing the cut-off frequency of the filter.

In the first instance, a Butterworth filter with cut-off frequency at 1.1 rad/sec was used. This only introduced a small amount of phase-lag to the signal and did not affect the motion greatly. The cut-off frequency of the all-pass filter was then selected between 1.4 to 0.3 rad/sec at a few discrete frequencies. The resulting r.m.s motions are shown in fig.8a,8b and 8c. The 0.3 rad/sec cut-off has produced the best overall performance compared to those resulting from higher frequency cut-off. Even so, this performance is only a slight improvement on the original unfiltered case. Although the rudder r.m.s. rate responses in fig.8c show little variation with different cut-off frequencies, there are in fact differences in the rudder response spectra especially near the roll natural frequency. The rudder response near the roll natural frequency is quite sensitive to the amount of phase-lead introduced.

To improve the feedback signal further, a Butterworth filter with a lower cut-off frequency was then used to suppress a wider range of the undesirable frequency. The cut-off frequency was located at 0.9 and 0.7 rad/sec. Again a selection of cut-off frequencies for the lead compensators were used to give varying degrees of phase-lead. The resulting r.m.s motions are shown in fig.9(a-c) and fig.10(a-c). In general, the motion amplitudes have been reduced further except with the phase-lead compensators having the lowest cut-off frequencies. At these frequencies, motion amplifications were evident. This was probably due to the over-compensation in the phase advance. The best performance was derived from the combination of Butterworth cut-off at 0.7 rad/sec and all-pass at 0.5 rad/sec (fig10a-c). Very similar resulting motions were also found in fig.9a-c with the phase-lead cut-off frequency at 0.3 rad/sec. However, looking at the rudder rate amplitudes, those in fig.10c would be more desirable as it is more effective at a larger range of wave angles. Judging from these results, it may seem possible to improve the performance further if the cut-off frequency of the butterworth filter is lowered still. However, this would very likely to incur complications as the cut-off frequency would

be too close to the roll natural frequency.

In fig.11a,b, a comparison is made of the filtered RLS with the RRS and RLS results from the last report (Tang[4]). Although the filtered RLS case has reduced the motions quite substantially compared to the unfiltered case, it is still not as effective as the RRS with normal rate feedback. The comparisons in terms of the response spectrum are shown in fig.12a,b.

The roll response near the natural frequency has been successfully reduced by the filters even to a level lowered than the RRS case. However, it is quite evident that at lower frequencies, motion amplification has been brought about by the resulting phasing of the filters. This is also apparent in the rudder response at these frequencies when filters have been used (fig.12b). One the whole, the rudder response has been improved with these filters to achieved lower r.m.s. motions.

Concluding remarks

It has been shown that low-pass filters can incur undesirable phase-lags into feedback signals, which will degrade the performance of rudder induced motion stabilisations. This phase-lag effect can be reduced quite substantially by phase-lead compensation using an all-pass filter, thus improving the effectiveness of the RLS strategy. Despite this improvement, the performance of RLS is still inferior to RRS with simple roll rate feedback.

References

- [1] Baitis E. & Schmidt 1989
Ship roll stabilisation in the U.S. navy
Naval Engineers Journal
- [2] Conolly J.E. 1969
Rolling and its stabilisation by active fins
T.R.I.N.A. Vol.111
- [3] Schmitke R.T. 1980
The influence of displacement, hull form, appendages, metacentric height and stabilisation on frigate rolling in irregular seas
STAR symposium, California

[4] Tang A. & Wilson P.A. 1991

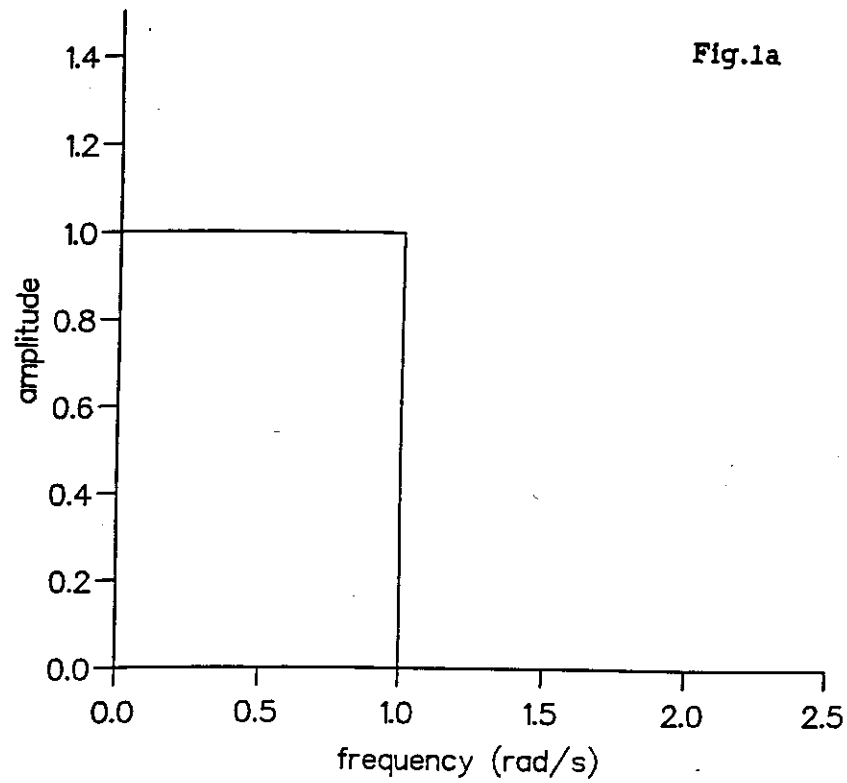
An investigation into L.F.E. stabilisation using the rudder
Ship Science Report

[5] Van Amerongen J. et al 1983

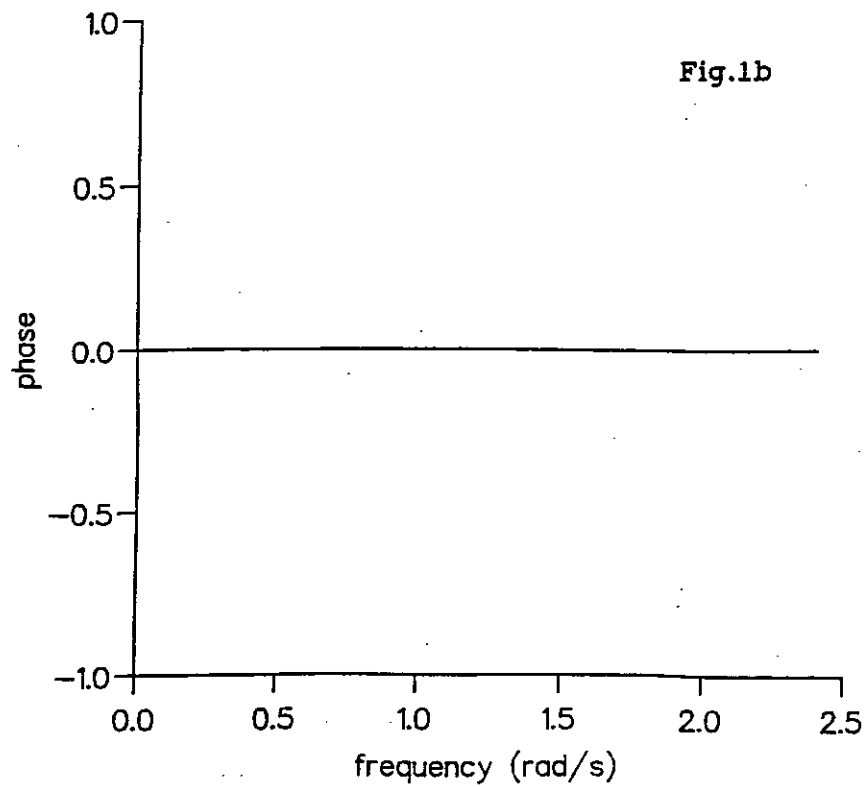
Roll stabilisation of ship by means of the rudder

Proceeding of the 3rd Workshop on Application of Adaptive Systems theory, U.S.A.

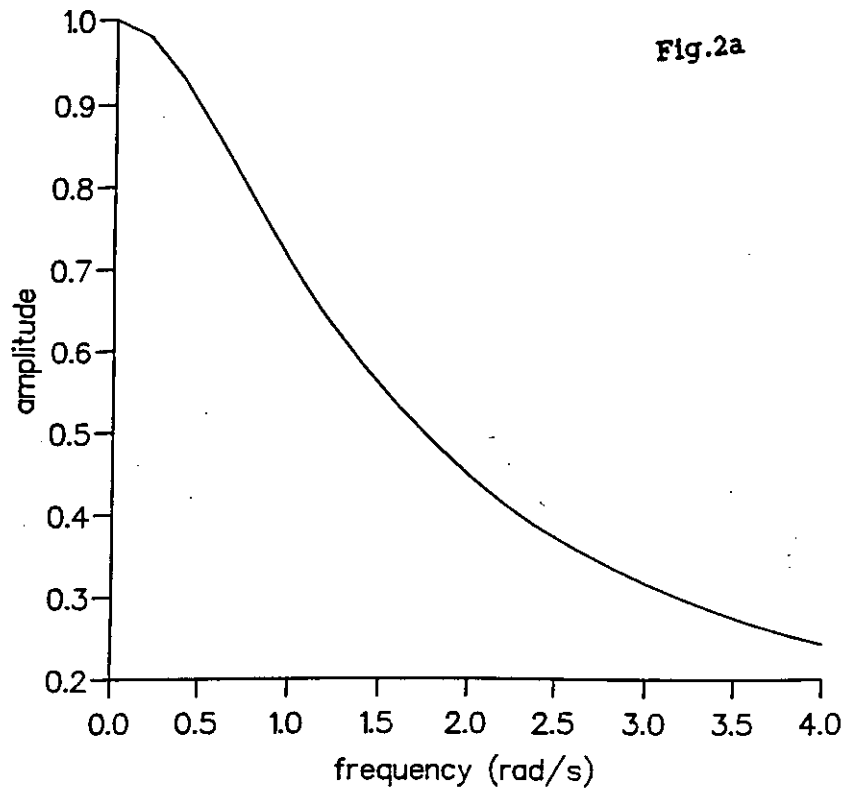
Response of an ideal low-pass filter



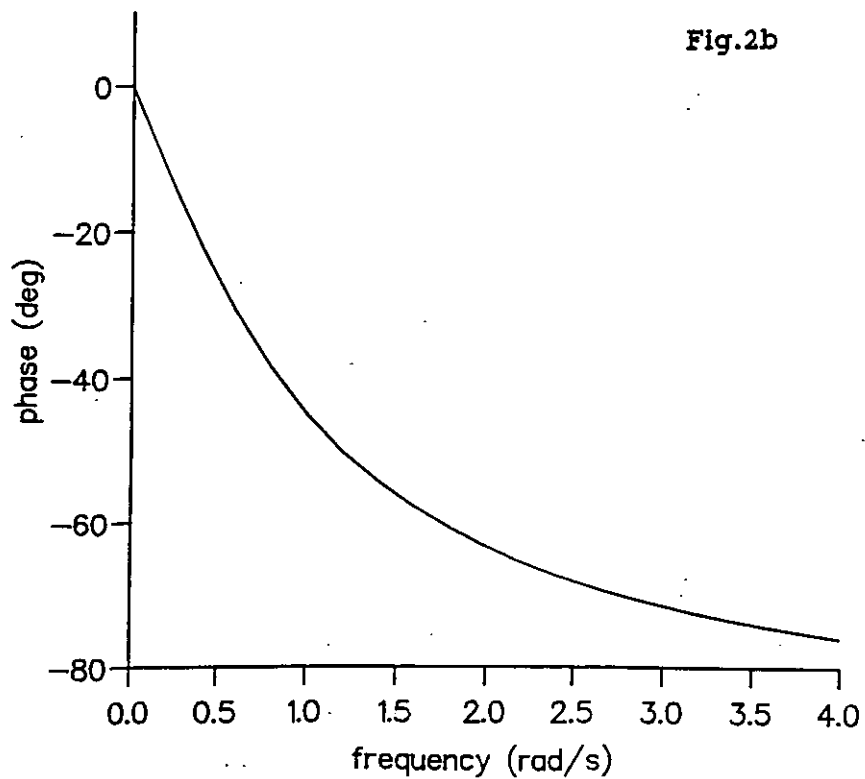
Response of an ideal low-pass filter



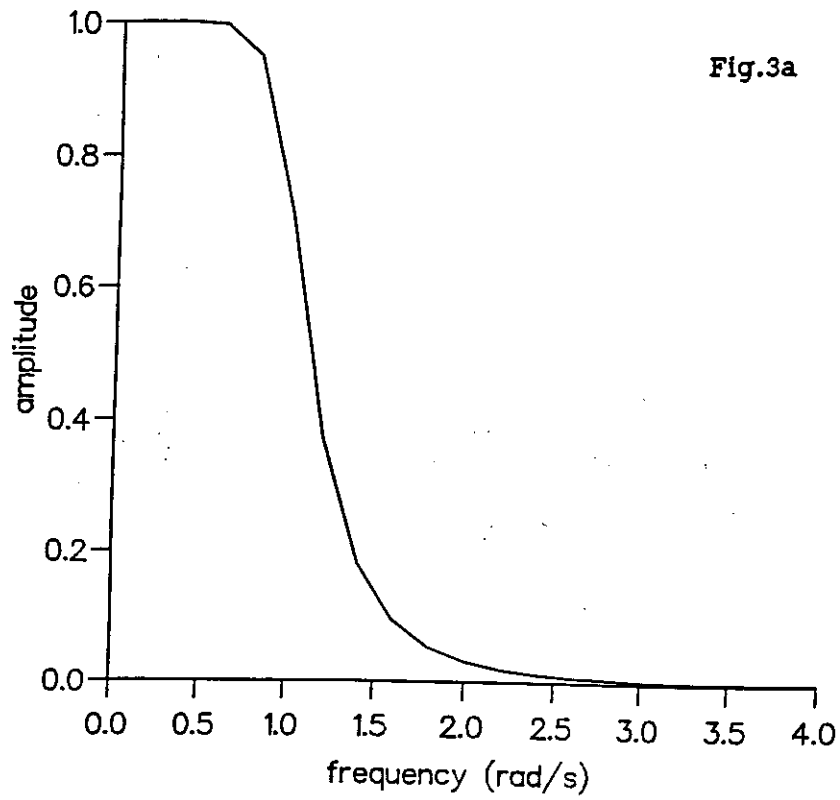
Response of a linear low-pass filter



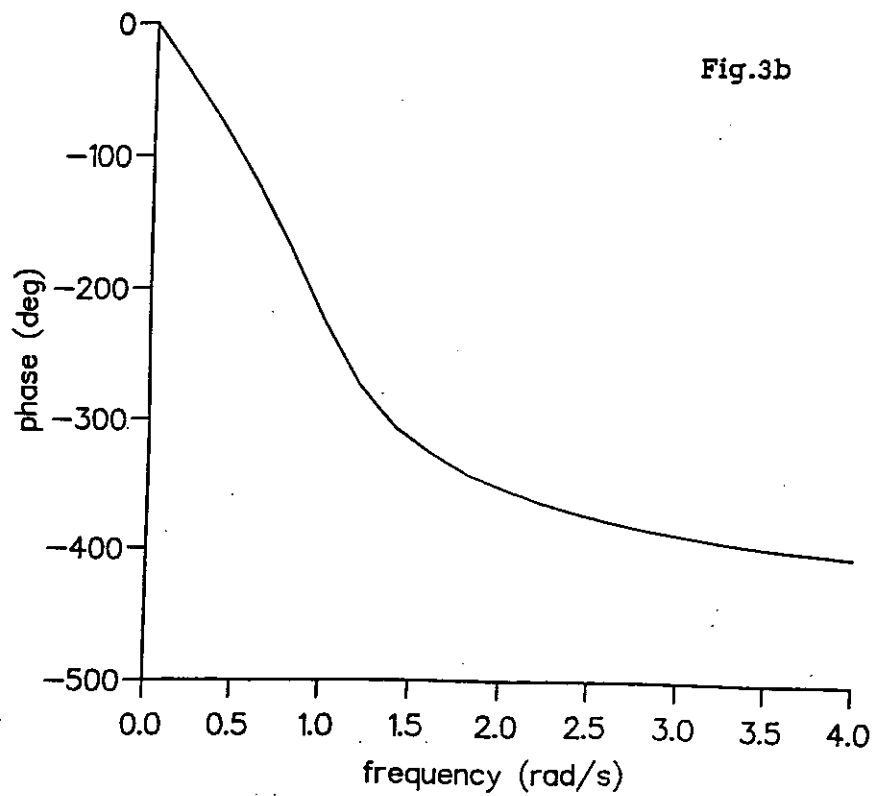
Response of a linear low-pass filter



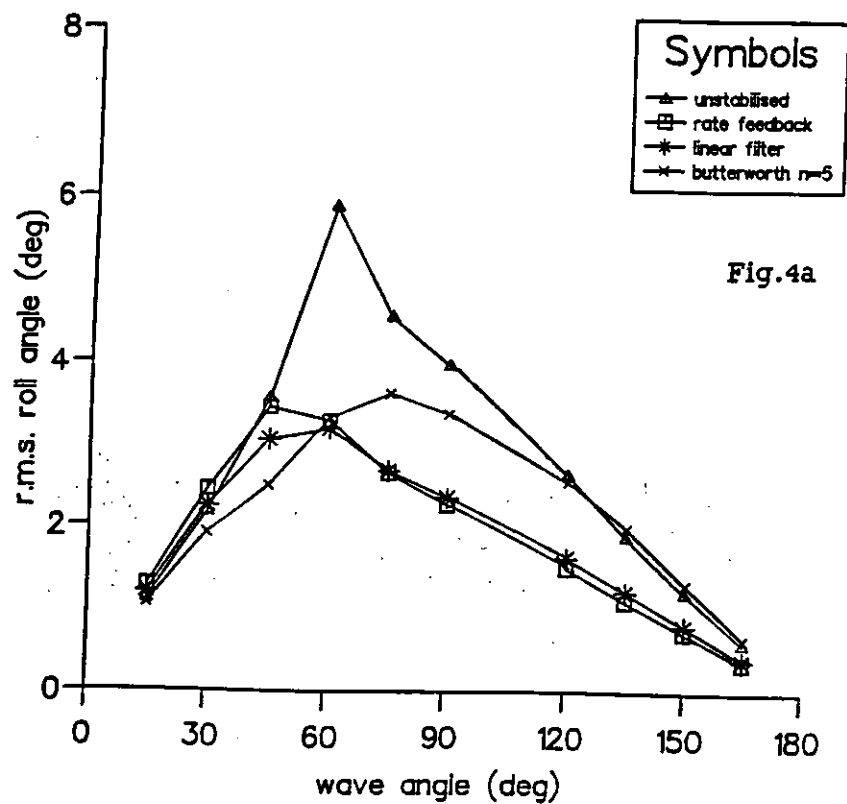
Butterworth $n=5$ filter response



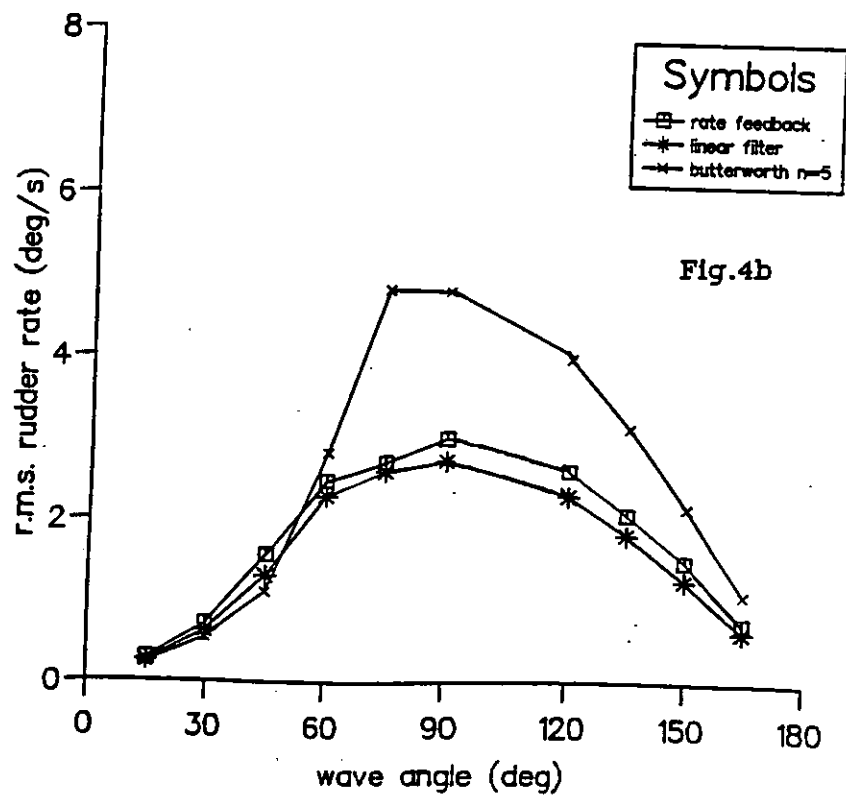
Butterworth $n=5$ filter response



Roll responses with filters



Rudder rate responses with filters



roll response with butterworth $n=5$ filter
(varying the cut-Off frequency)

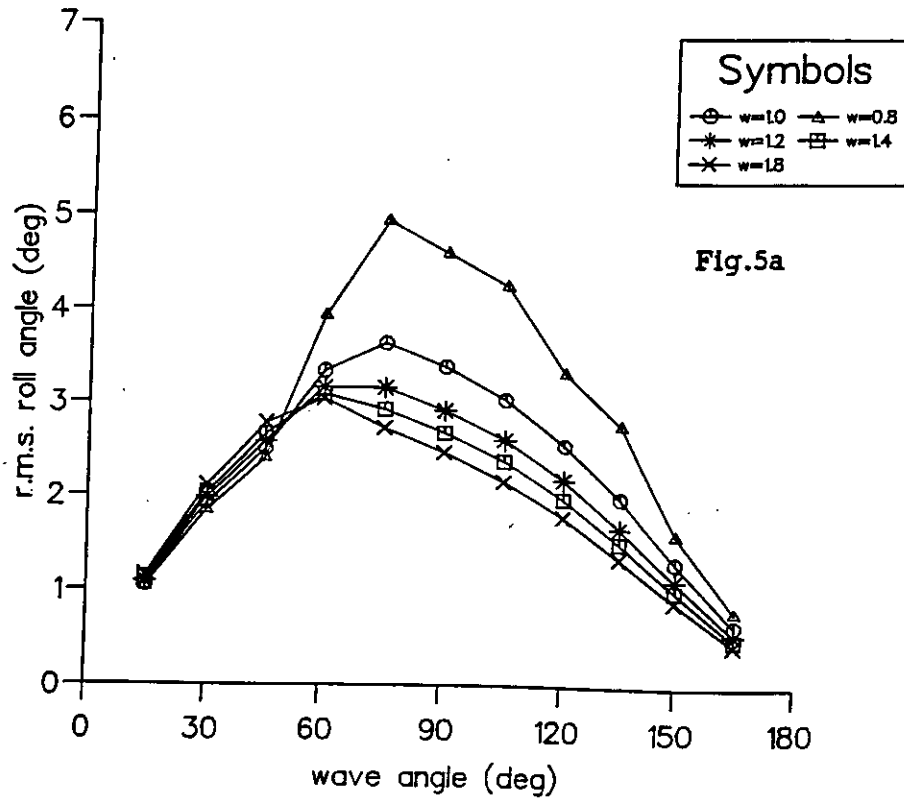


Fig. 5a

rudder rate response with butterworth $n=5$ filter
(varying the cut-Off frequency)

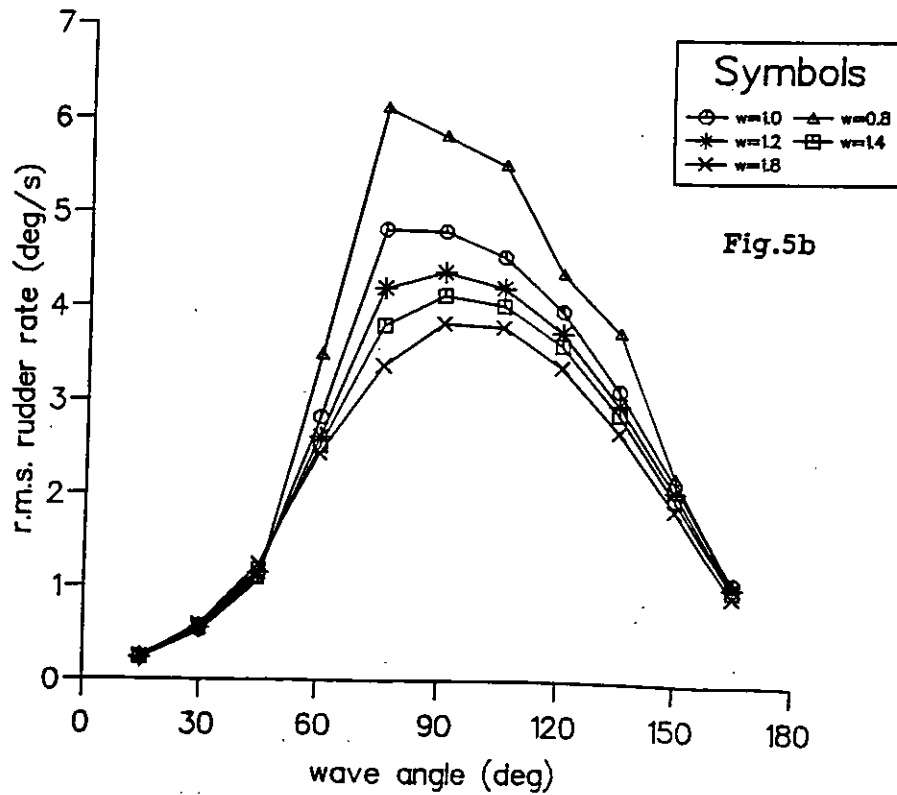


Fig. 5b

Response of a lead-compensation filter

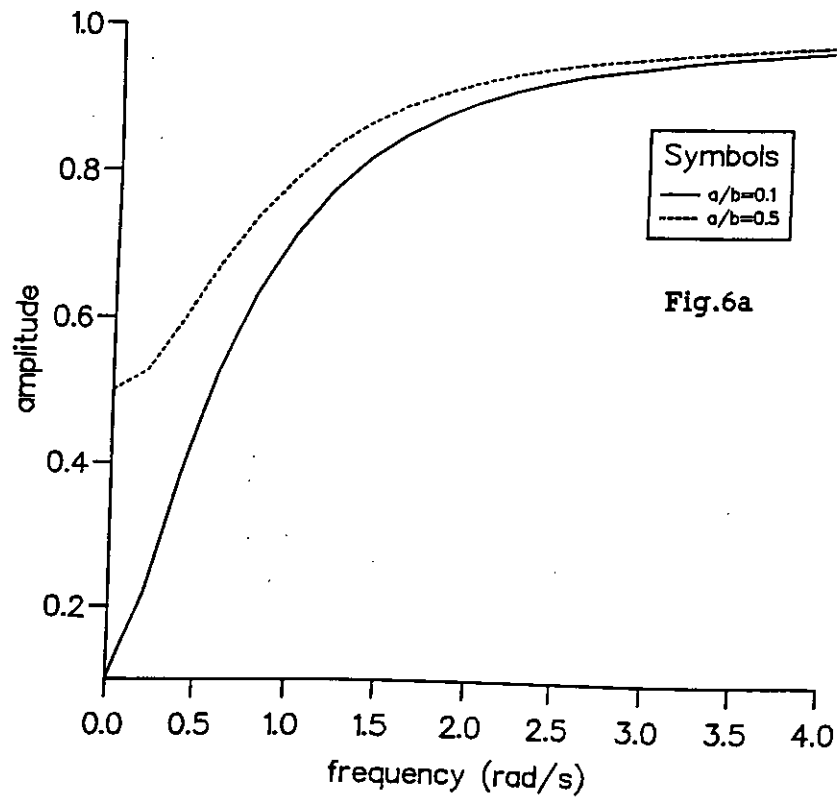


Fig.6a

Response of a lead-compensation filter

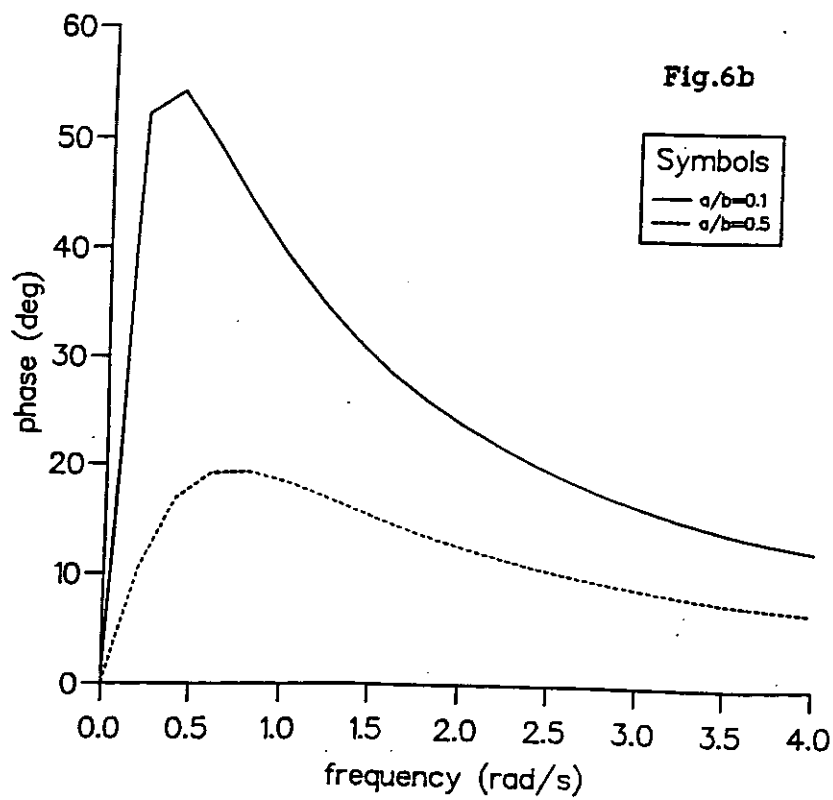
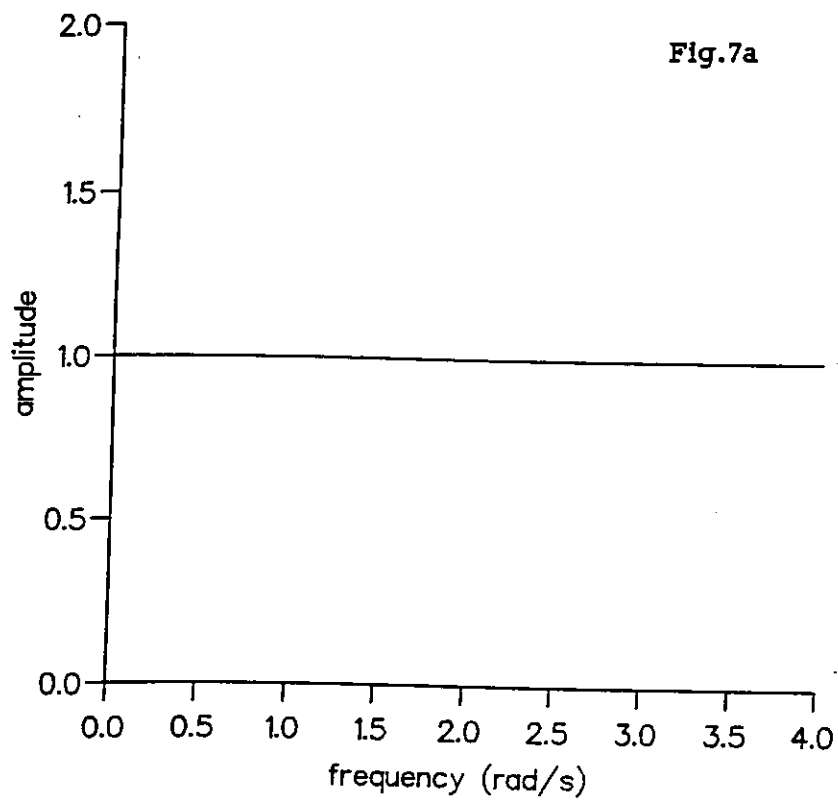
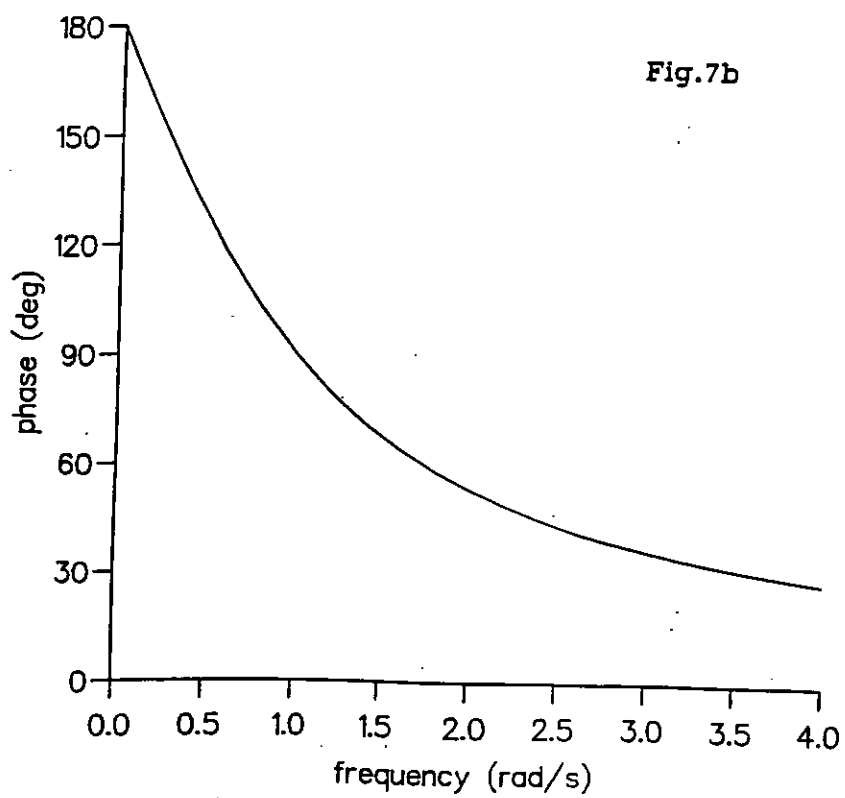


Fig.6b

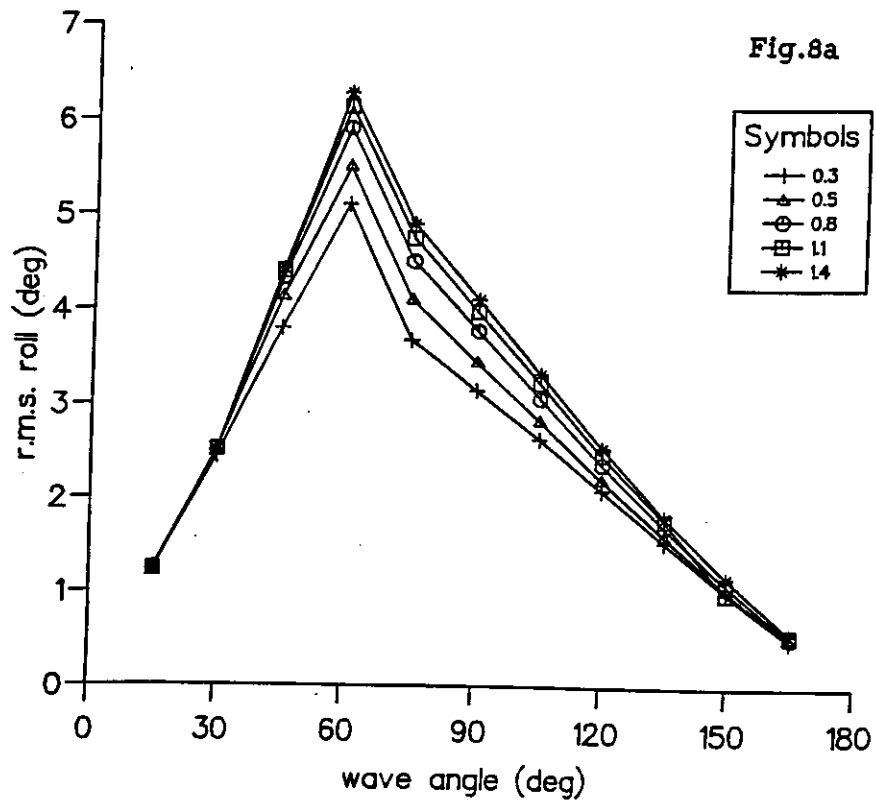
All-pass filter response



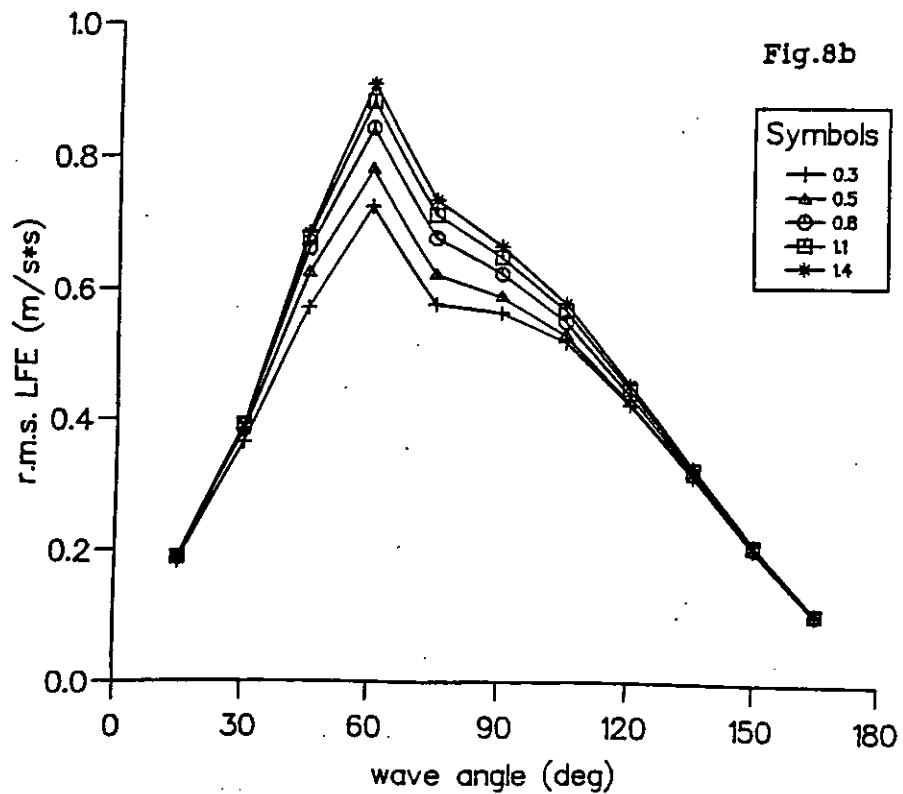
All-pass filter response



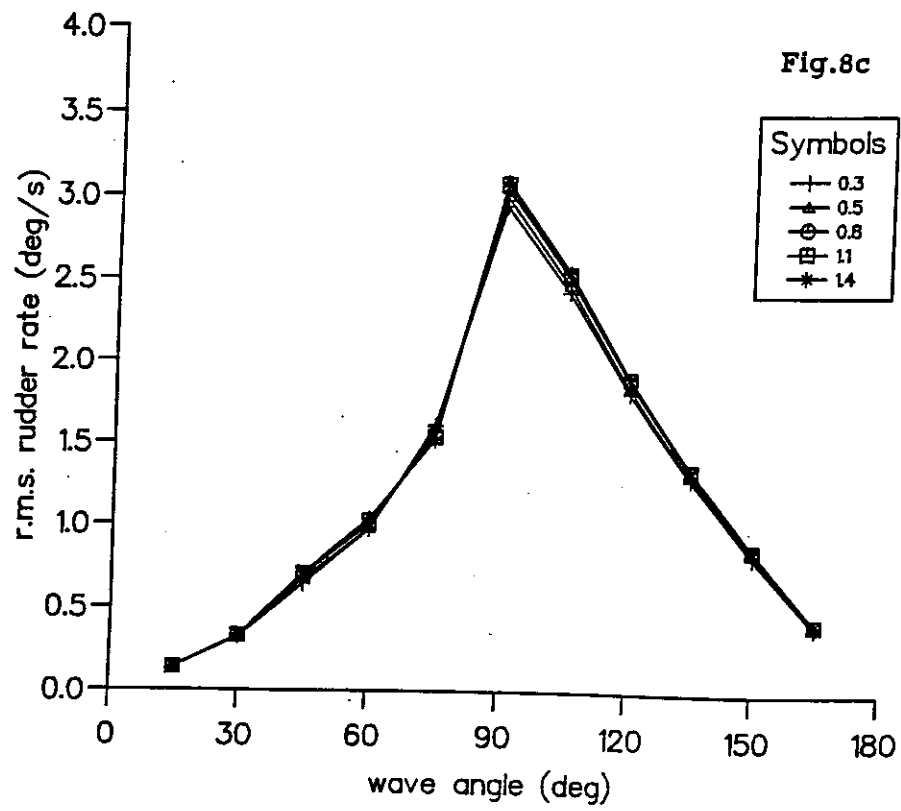
Roll response due to $B=1.1$ with all-pass filters



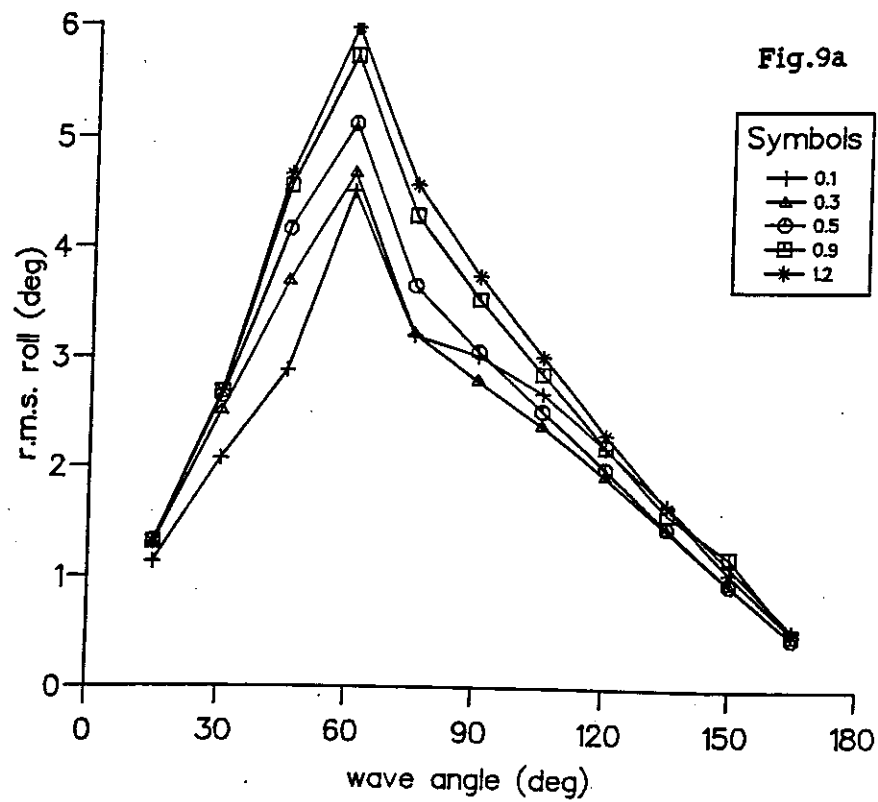
LFE response due to $B=1.1$ with all-pass filters



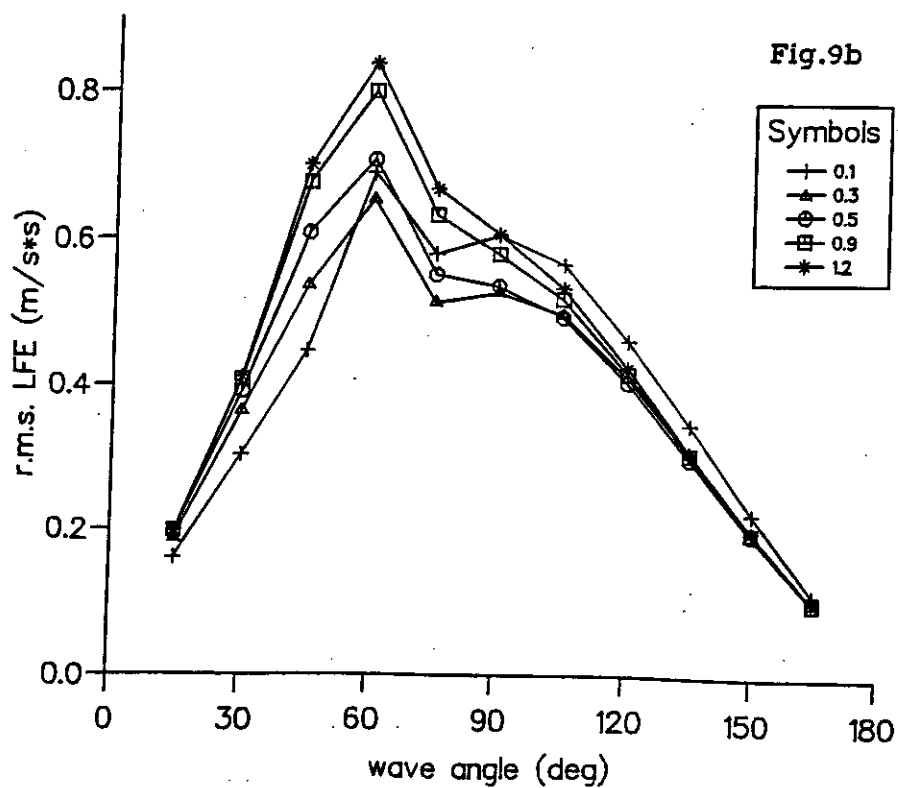
Rudder rate due to $B=1.1$ with all-pass filters



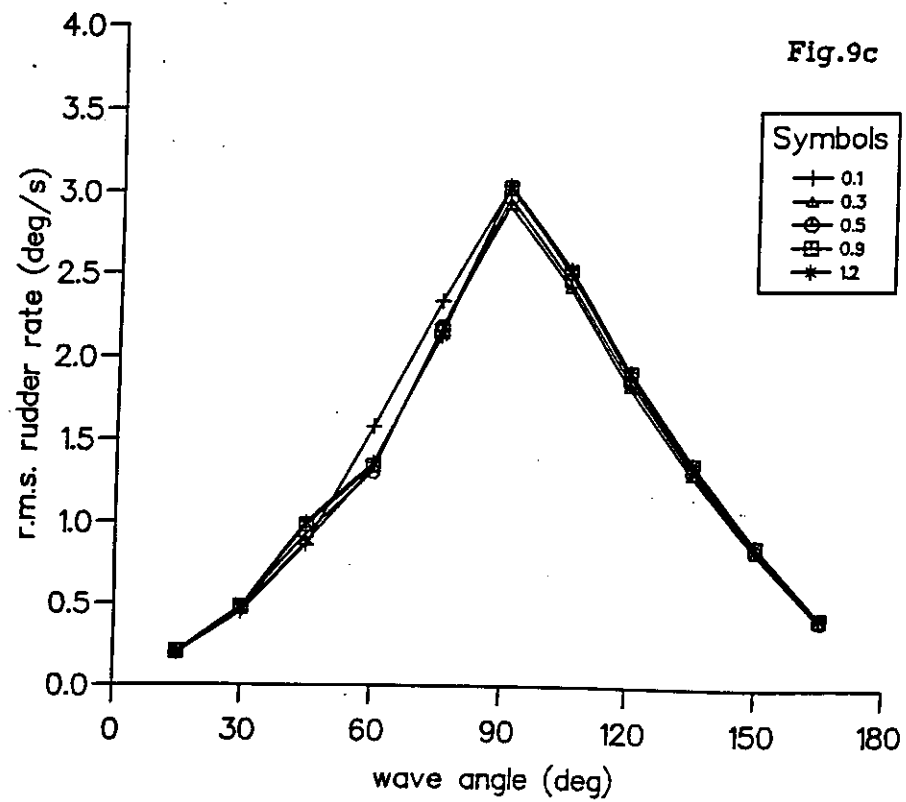
Roll response due to $B=0.9$ with all-pass filters



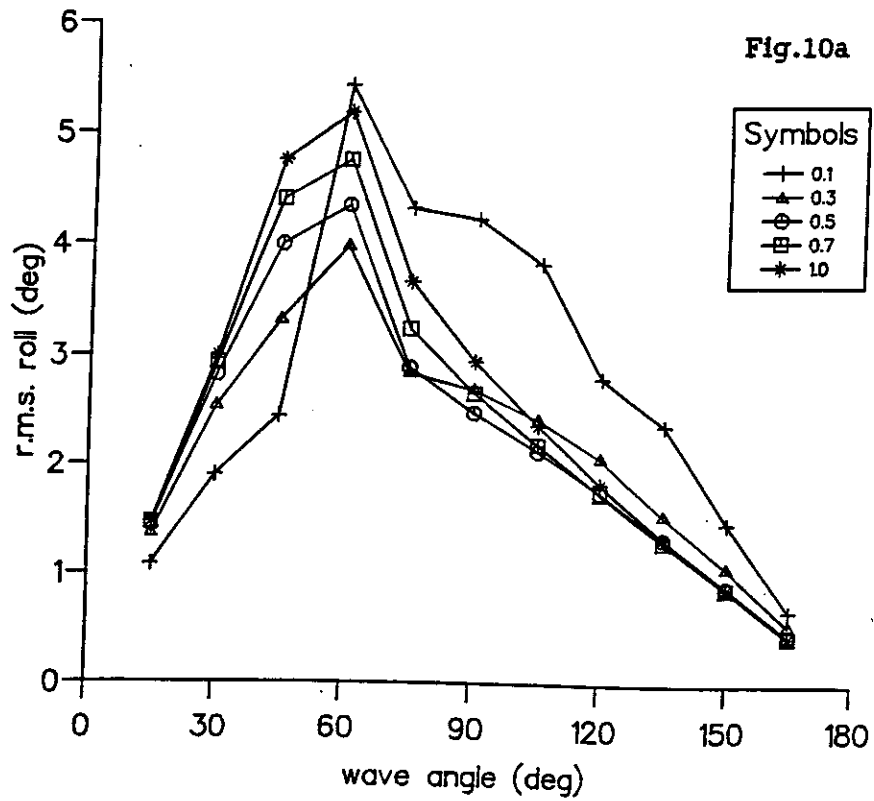
LFE response due to $B=0.9$ with all-pass filters



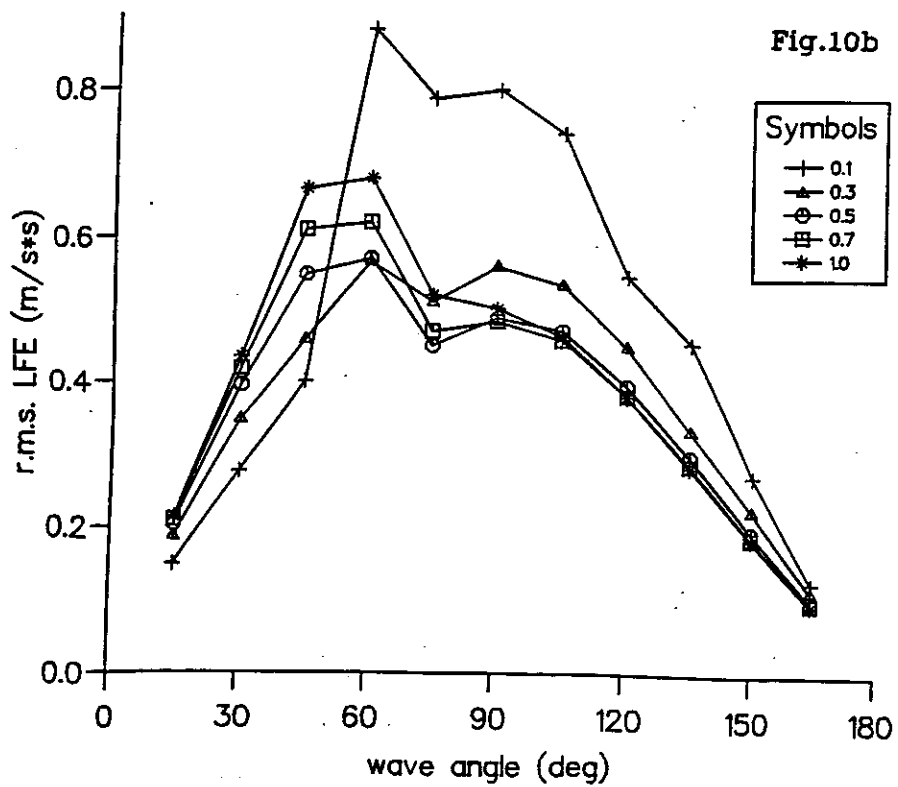
Rudder rate due to $B=0.9$ with all-pass filters



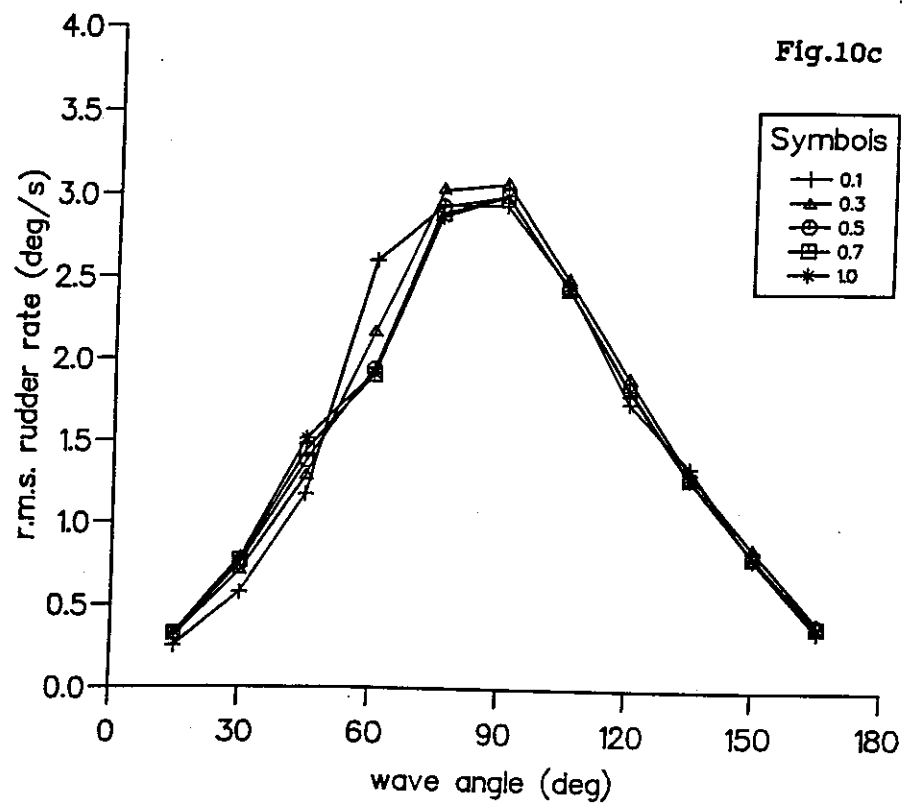
Roll response due to $B=0.7$ with all-pass filters



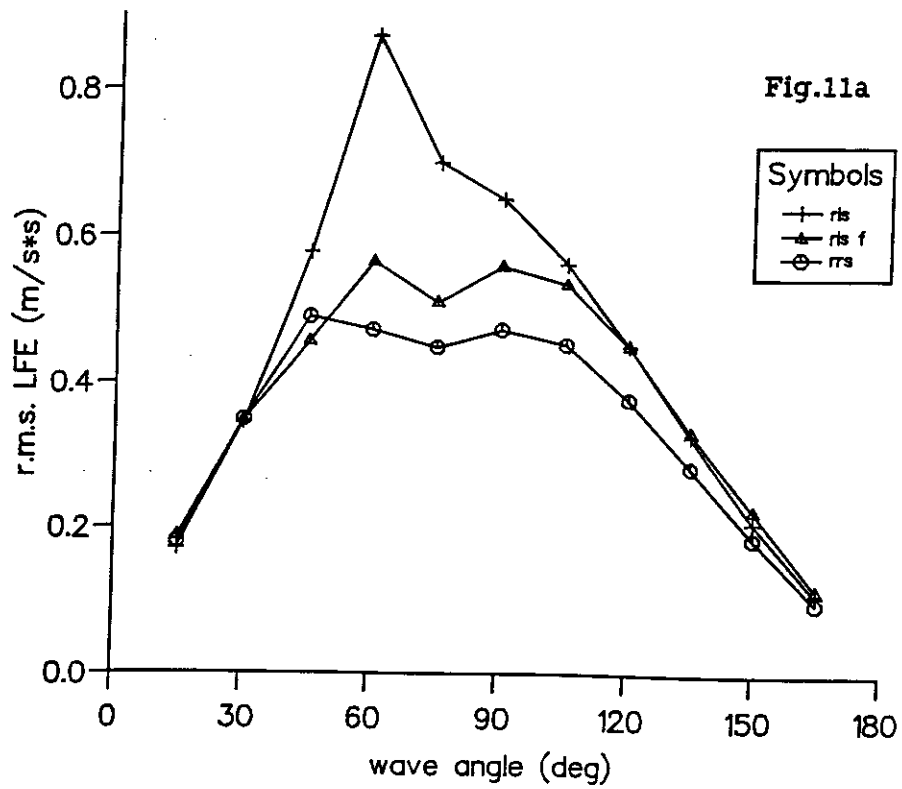
LFE response due to $B=0.7$ with all-pass filters



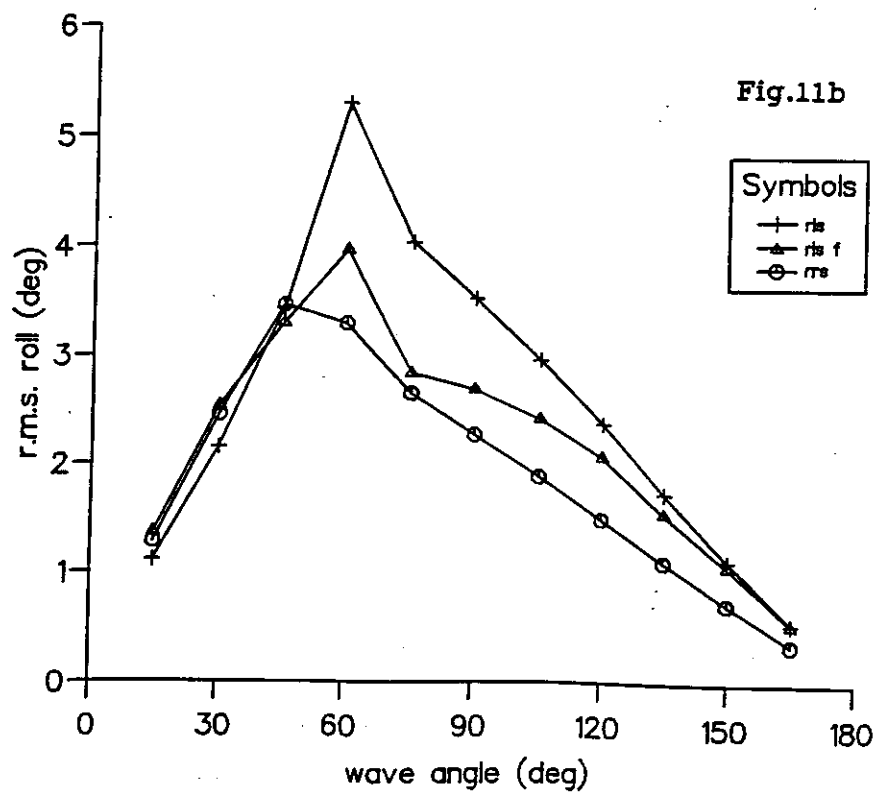
Rudder rate due to $B=0.7$ with all-pass filters



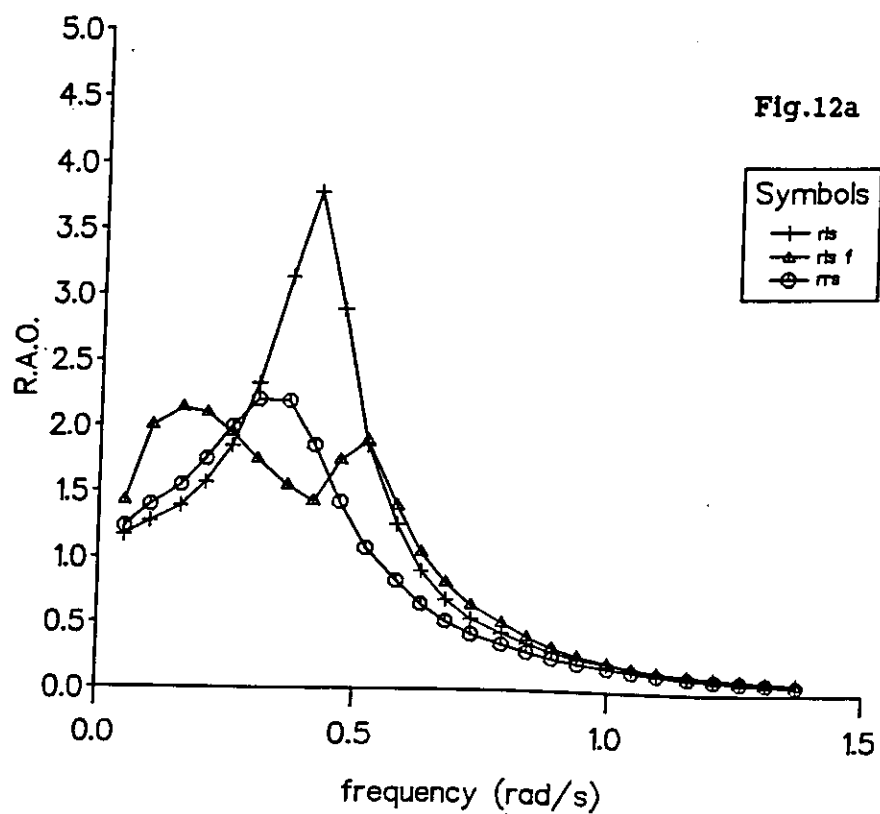
LFE response with and without filters



Roll response with and without filters



Roll response spectrum



Rudder rate response spectrum

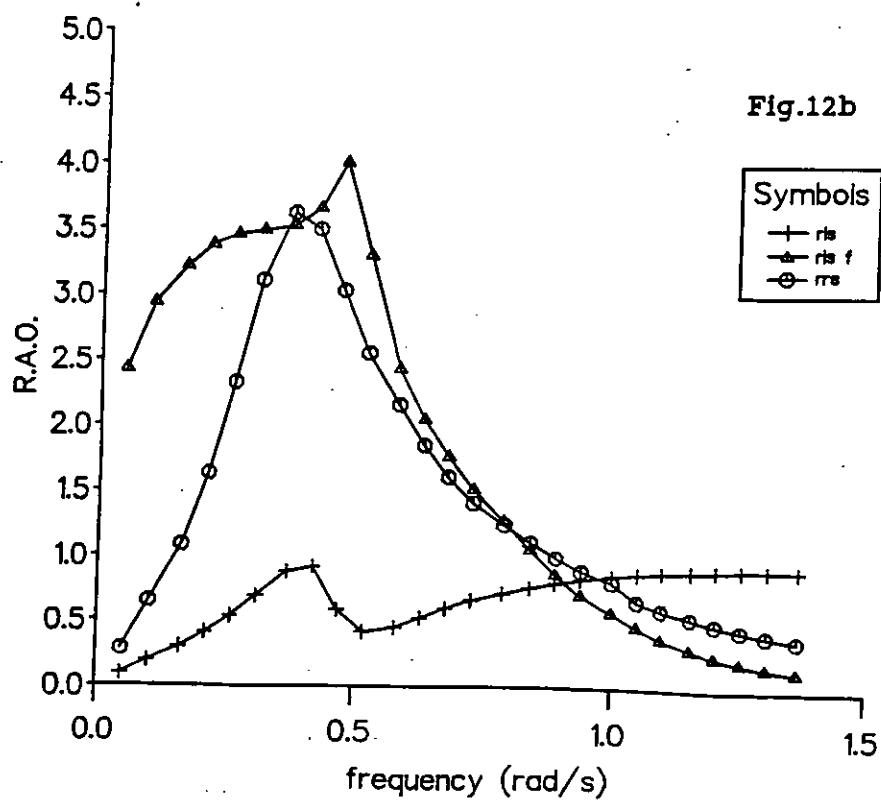
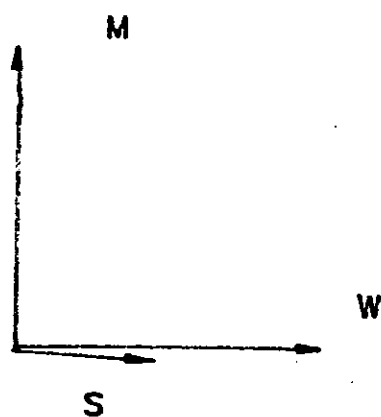
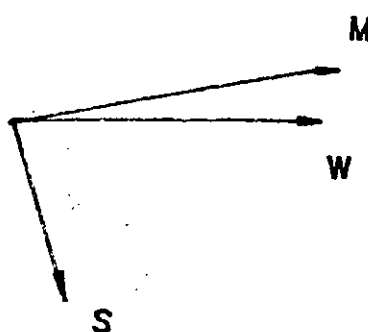


Fig. 1a-1c Vector diagrams for simple roll rate feedback stabilisation

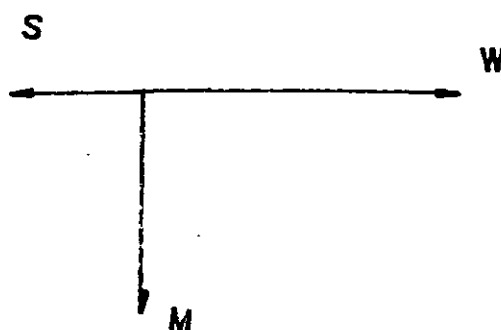


The vectors are not drawn to scale

(1a)
low frequency

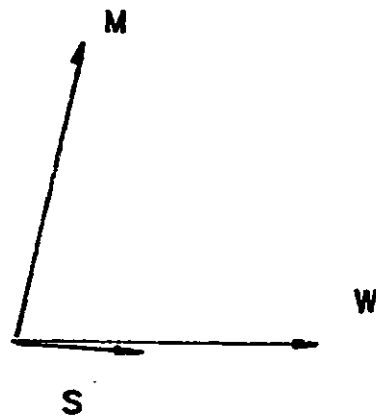


(1b)
near resonance



(1c)
high frequency

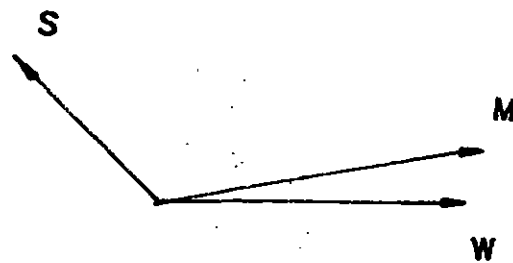
Fig. 2a-2c Vector diagrams for simple roll rate feedback with filter



The vectors are not drawn to scale

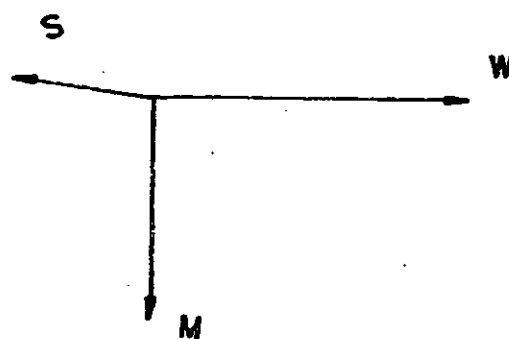
(2a)

low frequency



(2b)

near resonance



(2c)

high frequency

PART II

A/ LFE part I trials

A1/ Introduction

A forced roll/LFE trial was conducted on the 15th of June 1992 onboard HMS Lancaster. This was the first part of the LFE stabilisation trials, in which data for the motion and fin response were collected. At the same time, the sea-trial also provided an opportunity for the trial team to gain some working experience with the new fin controller as well as the crew members onboard ship. The motion data derived have been used to compared with the numerical simulations in this part of the report.

A2/ Trials procedure

The trials consisted of three parts:

- a/ the lurch test to locate the natural roll frequency,
- b/ the motion response over a range of forced roll frequency, and
- c/ the roll decay tests.

Originally, to perform the lurch test, two crew members were needed in the engine room to set the initial fin angles. Once a steady heel was achieved, the fins were discharged to their normal parked condition, which would excite the ship to roll at its roll natural frequency. However, due to the recording equipment failure and the demand on man power, this test procedure was abandoned. An alternative approach was tried. In this case, the ship was forced oscillated with the fins using square sine waves with the longest period (40 seconds) available in fin controller (CCU). Although the ship took longer than forty seconds to complete the decay motion, an estimate of the natural roll period should not be greatly affected. Unfortunately no useful data was derived from these tests. Due to the constraint of time, no further effort was made to obtain an estimation of the roll natural frequency.

The frequency response test was greatly enhanced by the built-in forced roll function of the CCU, which was found to be robust and easy to use. The procedure consisted of dialling in a sequence of requests on the console of the CCU, specifying the fin motions, then activating the requests and cancellations after a length of time. A typical example of the sequence is illustrated as follows:

31 20	forced roll period:	20 seconds (05-40 sec)
32 16	forced roll amplitude:	16 degrees (01-28 deg)
33 01	wave form:	sine
20 05	execute the requests	
20 11	cancel the requests	

(For the lurch test, the 33 01 was replaced by 33 03 for square waves.)

In general, more than ten cycles of motion were recorded for the subsequent analysis. As the resolution of the forced period parameter is one second, it is quite likely that the exact roll natural frequency cannot be selected.

For the roll decay tests, the ship was first forced oscillated near the natural roll frequency till a steady state was reached. The fins were then parked to allow the roll motion to die out. This was carried out with three different ship speeds, and the roll damping coefficients were derived.

In this trial, seven channels of time-history signal were recorded from the following devices: a three component accelerometer near the hangar, a lateral accelerometer near the workshop, the roll angle signal from the ship's gyro and the fin input/output signal from the CCU. The positions of the accelerometers are given in table 1 below. From these transducer time-histories, the amplitude and phase of the signals were derived. During each run, the rudder was amidships and the ship speed was 15 knots except for the case c above. The displacement of the vessel was 4248 tonnes.

Table 1 : Accelerometer positions

	X (m) from midship	Y(m) from C.L.	Z(m) above USK
3-component accelerometer (hangar)	21.44	0.35	10.30
lateral accelerometer (workshop)	4.92	-0.34	8.51

A3/ Results and Discussions

1/ roll data

The roll amplitude and phase comparisons are given in fig. a1 and a2. In fig.a1, there is a difference of about 7% in the natural roll frequencies and about 15-20% difference in the amplitude response near the resonance frequency between the predicted and the trials data. Apart from possible measurement errors, these differences could be attributed to the GM value assumed in the simulation, as the GM during the trial was not known. In comparison to the GM, these differences should be less sensitive to the 'errors' in the roll damping and the fin lift coefficients of the numerical model. Therefore, if the assumed GM value is higher than the true value, the natural frequency would be expected to be higher and the amplitude response lower, as is the case in fig. a1.

The phase variation with frequency in fig.a2 between the two sets of data follows a very similar trend. The relatively large difference at low frequencies should not be taken too seriously as these measurements are very sensitive to the sea condition, which was not totally calm. Also, being at night, no effort was made to run the ship in head sea conditions as the sea state was less than two. The main point to note is that at low frequencies, both sets of data show non-zero phase values. This suggests the presence of some motion interaction effects, which are probably caused by the sway forces of the fins.

On the whole, both the roll amplitude and phase response comparisons show good agreements. Despite having only one pair of fins, the forced roll response of this ship shows that this design is as effective as some of the older designs, such as those used in the Leander (wide beam) class, which were installed with two pairs of fins.

2/ lfe data

The LFE amplitude and phase response are presented in fig. a3 and a4. The overall trends in both cases are similar to the corresponding roll data. In fig.a3, the LFE amplitudes at the workshop (trial W) are slightly lower than those at the hangar (trial H). The difference is due to the difference of about 3m in their vertical positions, which gives rise to different roll accelerations. The measured LFE is predominantly due to the roll angle equivalent

acceleration, which accounted for about 90% of the measurements near the roll natural frequency.

Apart from a shift of π , the LFE phase (fig.a4) and the roll phase (fig.a1) are almost identical. As the accelerometer was calibrated with a negative signal for a starboard roll, the π shift is evident. The acceleration terms in the LFE signal did produce a difference of a few degrees to the roll case both in the trials data and the numerical simulation. This difference is more apparent at the low frequencies. It should be pointed out that, in deriving these phase responses, a difference of π was found in cases using the measured data.

In fig.a5, a comparison of the 'sway' accelerations calculated from two different methods is shown: $S(t)$ is by subtracting the roll equivalent accelerations from the LFE in the time histories, from which the r.m.s. value is derived, whilst $S(w)$ is the difference in their r.m.s values without phase corrections. Although the magnitude of these data is fairly small, their comparisons should still give some indication of their credibility. In most cases the $S(t)$ data differ from $S(w)$, which show more scatter. More importantly, the $S(w)$ approach gives negative values at high and low frequency. Therefore, to derive the r.m.s LFE data, as shown in Monk's paper (TRINA 1987), by simply adding the r.m.s roll and lateral acceleration terms together without proper phasing would lead to questionable results.

3/ fin data

Over the range of frequency tested, the magnitude of the fin angles were almost the same as the demanded angles of 16 degrees. With the highest frequency used (1.23 Hz), this demanded amplitude was too high, which resulted in very sluggish performance. In this case, a fin demand of 13 degrees was used. The phase lag incurred by the CCU and the hydraulic system on the fins is shown in fig.a6. To simulate part of this phase response, the hydraulic system of a Type 22 frigate was assumed i.e. $a_1=1.0$, $a_2=0.318$ and $a_3=0.0253$. To account for the CCU system, the following data has been used in order to match the measured data: $a_1=1$, $a_2=0.1$ and $a_3=0.05$. The sum of these phase angles formed the fitted line in the figure.

4/ roll decay tests

Three speeds were used for these tests: 15, 18 and 22 knots. Unfortunately, the time-history for the 22 knots case was not good enough for analysis. The roll decay coefficients for the 15 and 18 knots cases were 0.126 and 0.136 respectively. The corresponding

estimated natural roll frequencies were 0.616 and 0.61 Hz. Judging from these figures, the motions should not differ greatly within this speed range.

B/ LFE Signal Conditioning

B1/ Design history and background

The original specifications for the LFE signal to the CCU (quoting from Brown Brother's proposal) are as follows: a synchro input would be used and the signal should be about 14 bits. This was all the design information that was provided by Brown Brothers Ltd. At a later stage, some additional information about the components required for generating such a signal were also given during discussions over the telephone, but on the whole, Brown Brothers was rather reluctant to be very specific. This lack of information has introduced additional difficulties to the design of the LFE signal conditioning. Nonetheless, a design was developed which was outlined in the last report.

During the visit to Brown Brothers, the hardware was briefly put to test. It was found that the fin response to the accelerometer signal was very stiff. Apart from this, no other undesirable effects were found. Two main reasons have been put forward to explain the stiff response. Firstly, the resolution of the system was restricted by the 14 bit ADC chip. The CCU has a resolution of 10 degrees per revolution and a maximum range of ± 30 degrees. This means that a 16 bit ADC would be more appropriate as it allows for more than two revolutions in the synchro output. Secondly, the CCU is only tuned for a frequency around the roll natural frequency and a high frequency input signal would saturate the response. Therefore, moving the accelerometer by hand as was done during the test could have caused such a stiff response. Apart from these two points, some additional information about the CCU system on the whole was also deduced from the discussions during the test. To satisfy these additional criteria, modifications to the original design were required.

B2/ Design modifications

Fig.b1 illustrate the signal path for LFE. Whilst the overall signal path is the same as the one described in the last report, modifications to the individual circuits have been made to suit the 'new requirements'. A brief account of these modifications are outlined below.

The band-pass filter in fig.b2 has a bandwidth between 0.05 to 1 hz as compared to a bandwidth of 0.002 to 10 hz in the old circuit. This reduction in bandwidth is to eliminate

further the unwanted signals, especially those at high frequency. However, adjustments may be needed if the phase lag associated with this new bandwidth was found to be higher than expected. After filtering, the voltage of the signal has been adjusted to about 2.7 volts, which corresponds to about 31 degree/rev in the Digital to Synchro (D to S) output. Fine adjustment would be needed to tune it down to 30 degree/ rev with the CCU. The voltage gain has therefore been made adjustable for this purpose. The time base circuit in fig.b3 is effectively the same as before. However, to accommodate the new 16 bit ADC chip, some fine tuning of the circuit has been carried out. The conversion frequency is still about ten times faster than the CCU.

The main modification of the whole LFE unit is to replace the 14 bit with a 16 bit ADC. The sole function of this 16 bit ADC chip is to provide two extra bits, which work as counters for a 14 bit signal. These two extra bits are not actually used in the main circuit. By allowing the digital signal to clock up twice, they can provide up to eight revolutions in the D to S output, whilst the digital signal is still of 14 bit accuracy. The new circuit for this chip is given in fig.b4. As the CCU only has a range of six revolutions corresponding to +/- 30 degrees of roll, the two extra revolutions from the 16 bit chip would be ignored, should the roll amplitude be higher than 30 degrees.

A wiring diagram for the different circuit boards is given in fig.b5. A test circuit board has been included in the unit to facilitate future testings. The circuit boards are housed in an aluminium rack as one complete unit, with one cable coming in from the accelerometer and one cable going out to the CCU. The cabling for the accelerometer and the D to S is shown in fig.b6.

At this stage, the whole unit has been tested and trimmed to the requirements available. Bench tests with the CCU will be needed to verify these modifications. Adjustments may be required to fine tune the unit for the sea-trials.

C/ CCU tests

A mechanical oscillator, which serves as a roll table, has been designed and constructed. The main purpose of this oscillator is to provide a means to generate known signals at a range of frequencies and amplitudes with a transducer, such as a potentiometer or an accelerometer, suitable for the CCU. This would allow the following objectives to be met in preparation for the sea-trials:

- a/ check the modifications described in the last section thoroughly over the range of frequencies of interest,
- b/ establish a procedure for setting the CCU gains for the sea-trial,
- c/ assess the gains derived for LFE stabilisation,
- d/ compare the fin response due to simulated roll and LFE signals.

The design of the oscillator was based on a scotch yoke mechanism, which has been used widely for producing sinusoidal oscillations for ship motion studies. However, in order to simplify the driving mechanism, a tangent oscillator was adopted. Therefore, above ten degrees of amplitude of oscillation, the generated signal would depart progressively from an exact sine wave. The oscillator proposed should have a frequency range between 0.2 to 0.05 Hz (5 - 20 sec) and an amplitude range between about 4 to 30 degrees. A d.c. motor has been used as the prime mover in the oscillator. The electronic circuits required for controlling the frequency of excitation and for interfacing the transducer signals to the CCU have been designed and constructed as an integral part of the mechanism.

An overall view of the mechanical design is given in fig.c1. This mechanism has been constructed and preliminary tests show that it performs well between oscillation periods of 5 to 16 seconds. Below 16 seconds, the mechanism does not run smoothly as there are slight mis-alignments in the set-up. In time, the system should be able to work down to 20 seconds after a good run-in. Also, at these low frequencies, the motor torque is low. Therefore, a simple voltage controller has been designed to cope with the variation in the loading. This is accomplished by velocity feedback from an optical encoder mounted on the drive-shaft of the mechanism. The circuit design is given in. fig.c2. To facilitate the selection and the determination of the test period, a display unit for the oscillation period has been included.

The circuit diagram for this unit is shown in fig.c3.

To simulate the test signals for the CCU, an accelerometer and a rotary potentiometer are mounted on the rotating arm of the mechanism. Signals from these transducers are fed into the LFE unit, which is interfaced to the CCU. By varying the amplitude and frequency of the oscillator, the fin responses due to these two input signals are then compared, which would give an indication of the LFE stabilisation strategy. Likewise, the most desirable gain setting could be selected for LFE.

For item d mentioned above, it was assumed that the 'sway' terms in the LFE would be about 30% of the roll angle and about 90 degrees forward in phase. This simulated LFE signal would be more representative of the LFE in a seaway than a pure sinusoidal signal. The phase angle and the signal amplitude can also be varied to give different combinations of a simulated LFE demand. The circuit diagram for this phasing is given in fig.c4, which is basically a modified all-pass filter. The accelerometer signal from the oscillator will be fed into this circuit first before connecting to the CCU.

The above plan shall be carried out as soon as the CCU at Sultan is available for testing.

Fig. a1

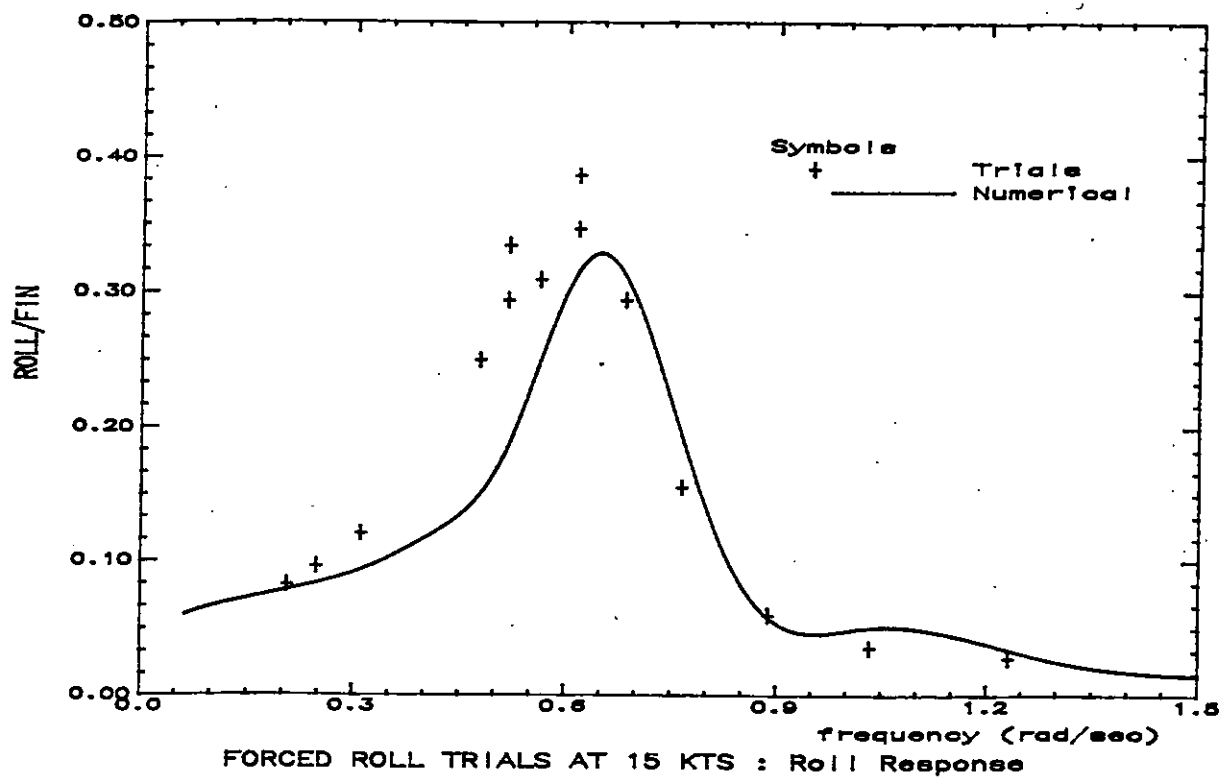


Fig. a2

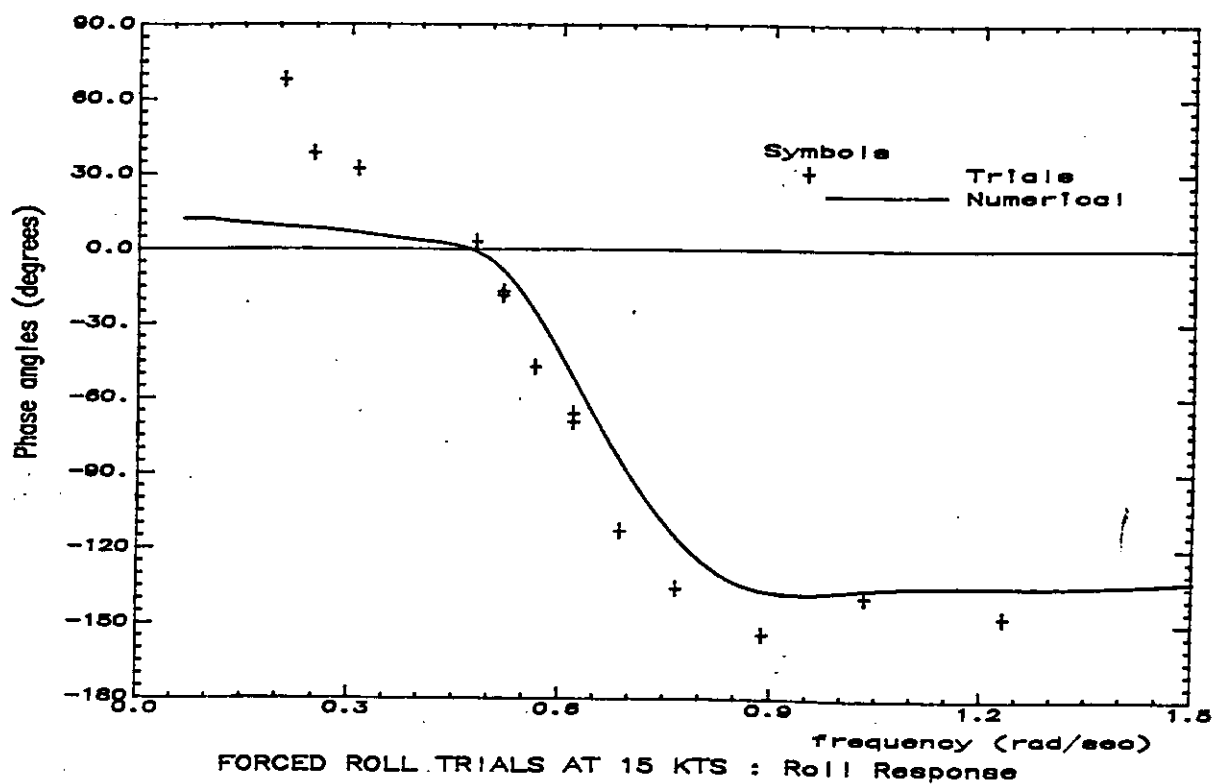


Fig. a3

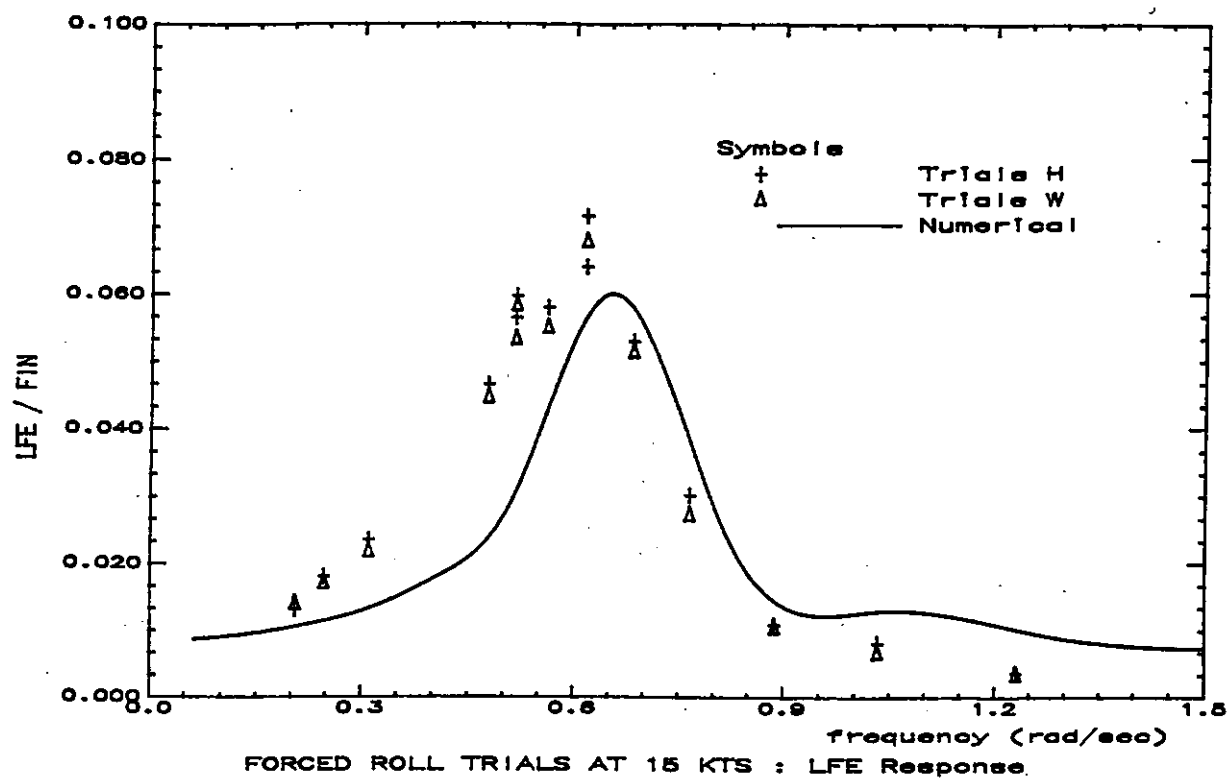


Fig. a4

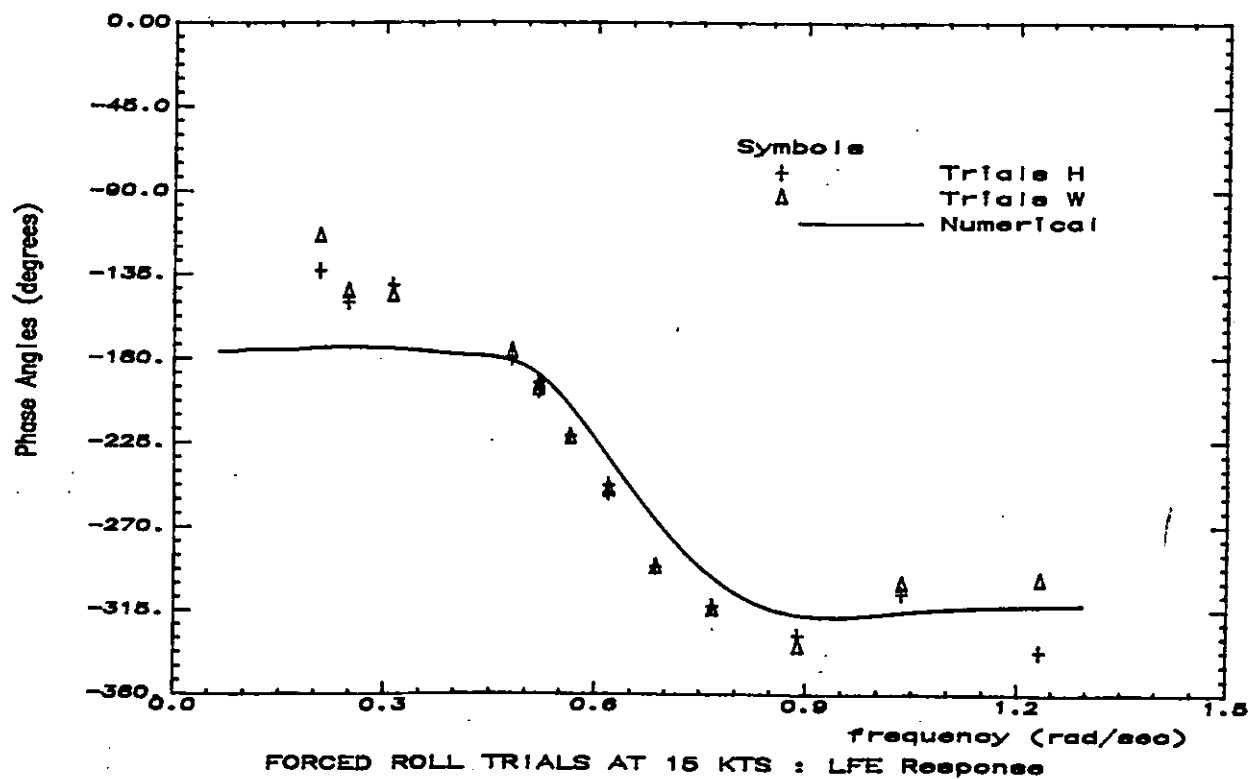


Fig. a5

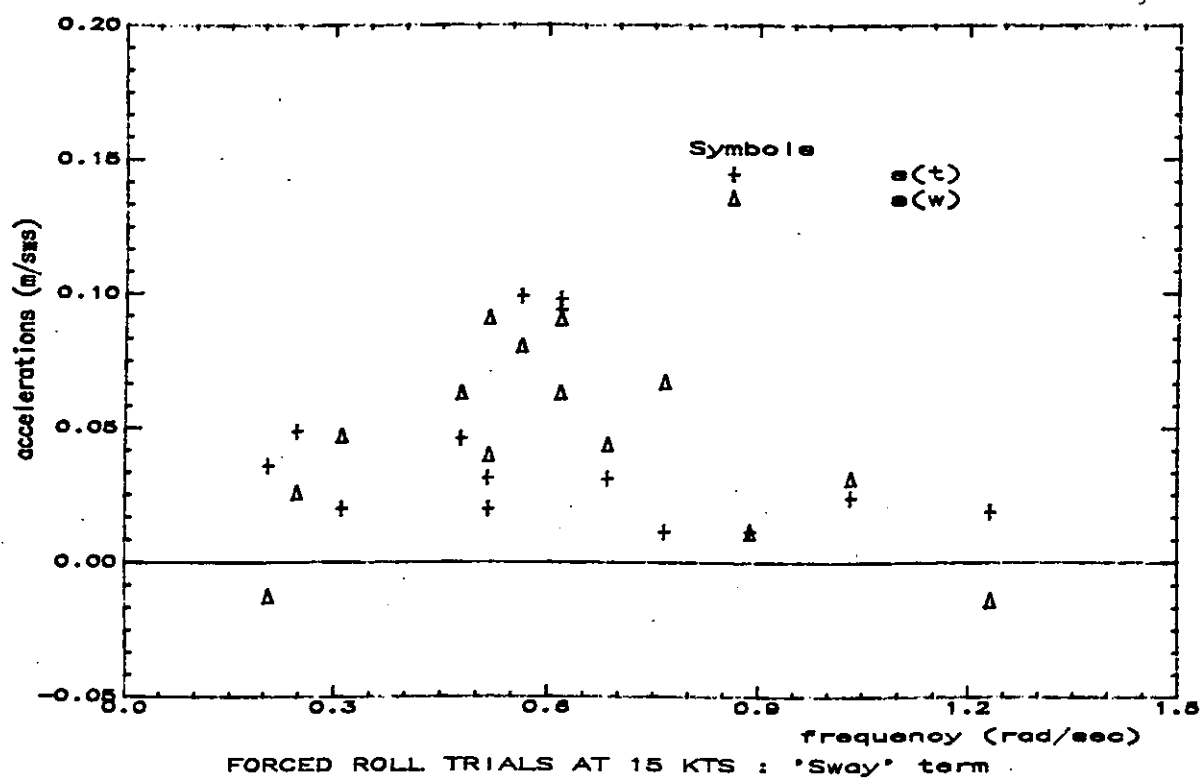


Fig. a6

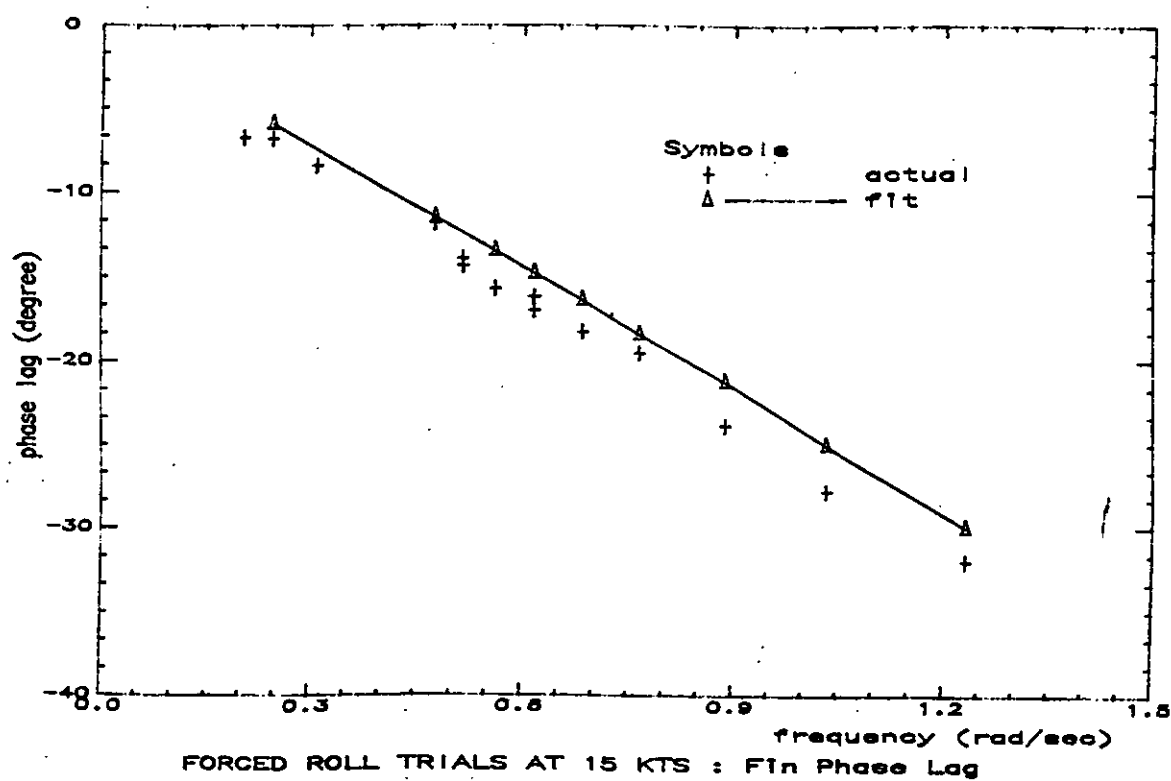


Fig. b1

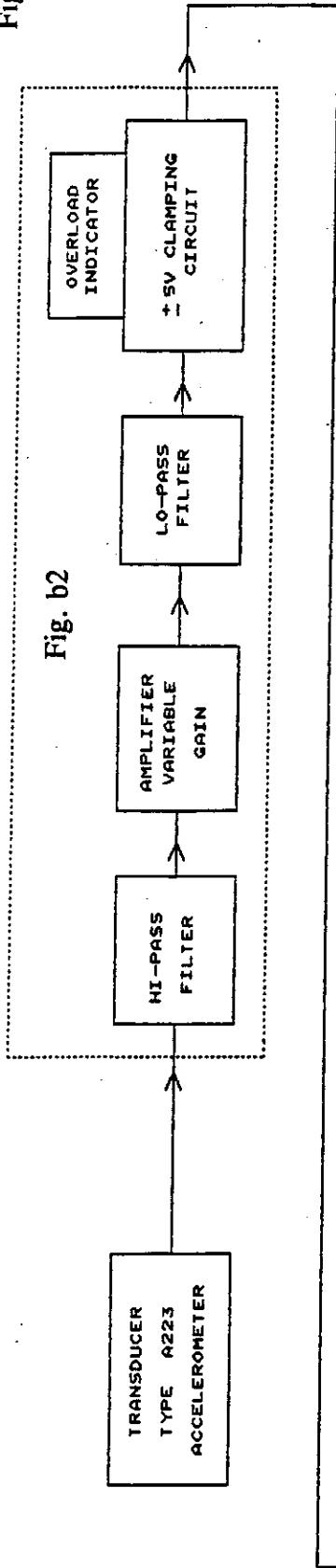


Fig. b2

Fig. b4

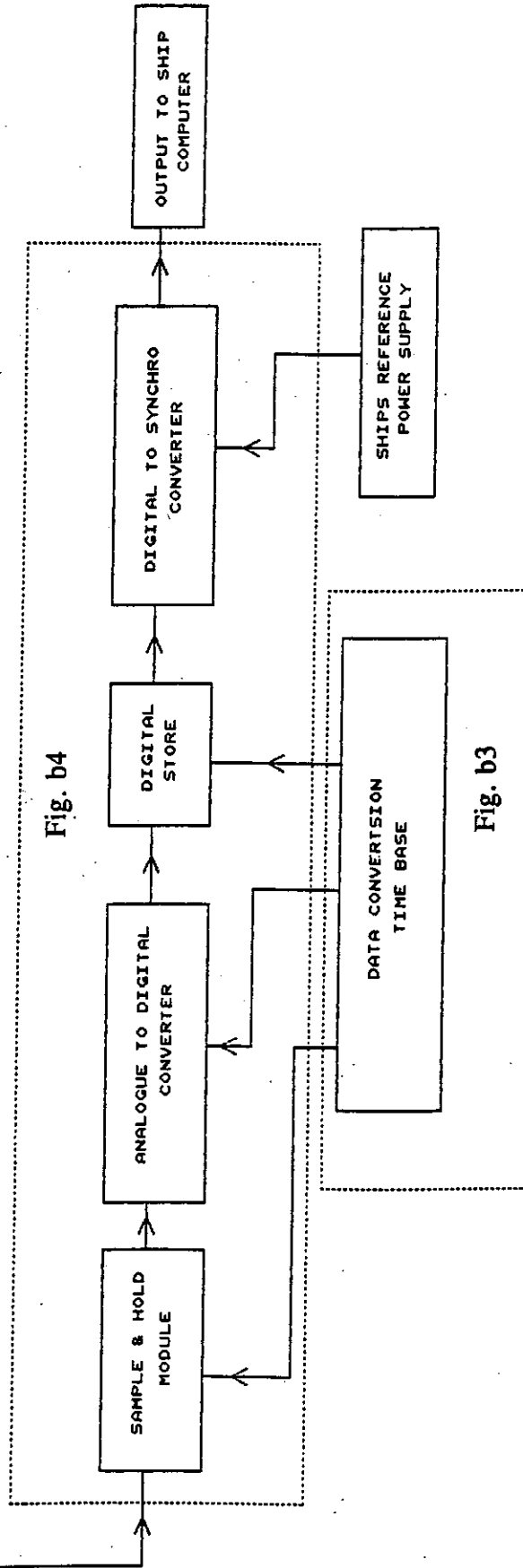
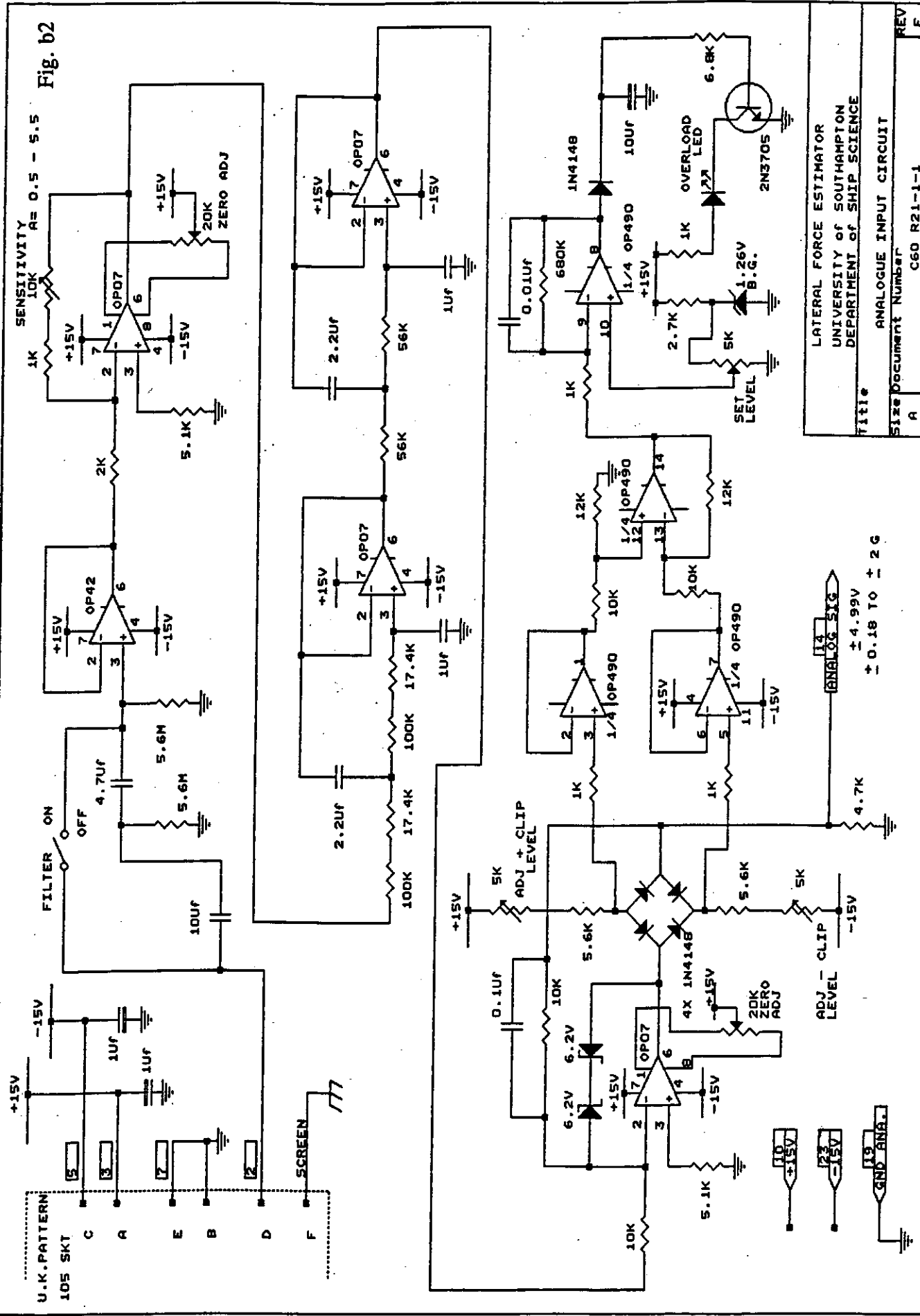


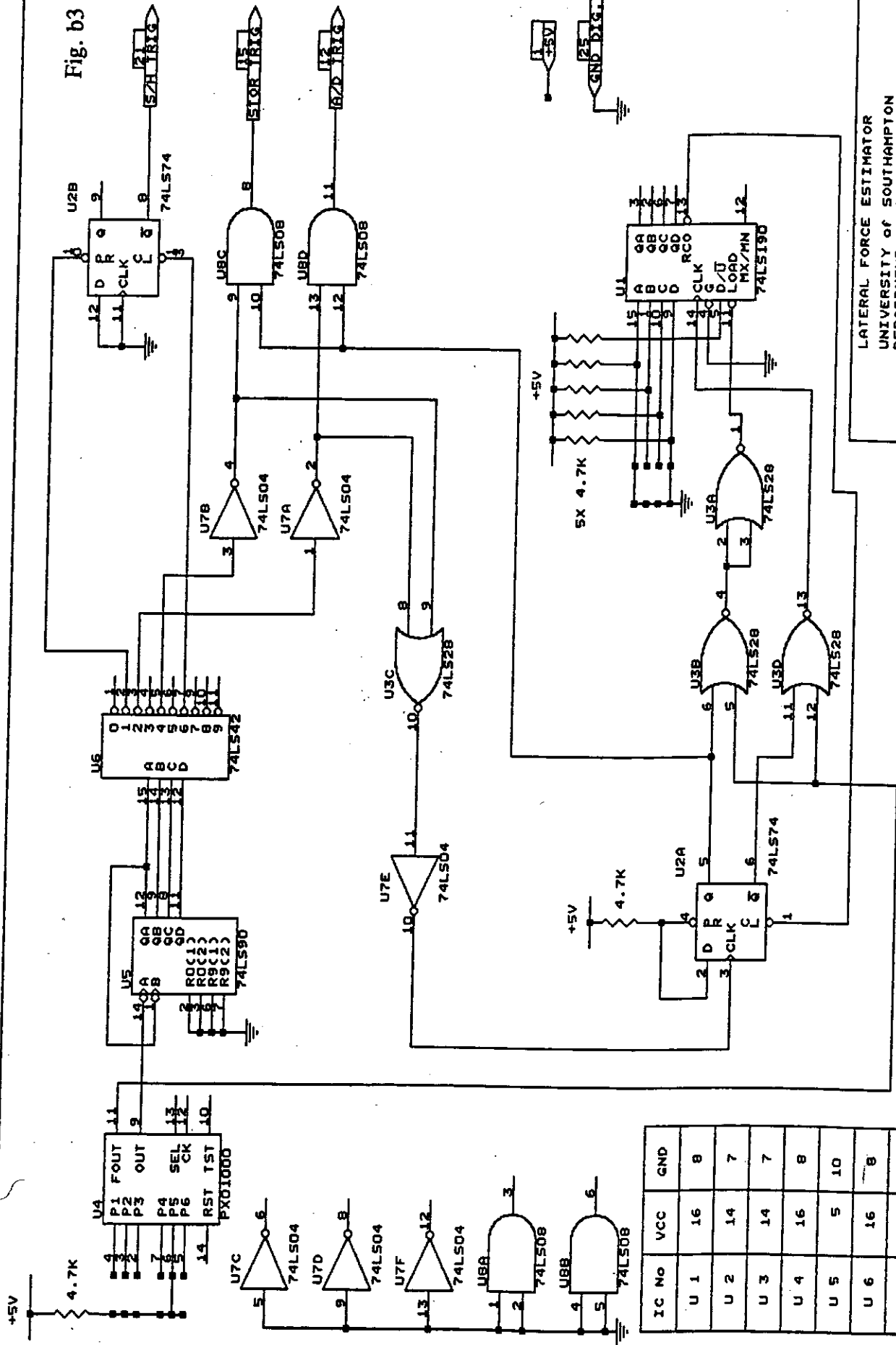
Fig. b3

LATERAL FORCE ESTIMATOR	
UNIVERSITY of SOUTHAMPTON	
DEPARTMENT of SHIP SCIENCE	
Title	
Size	Function Diagram
Document Number	C60 R2J-1-00
REV	
Date:	Sheet of



LATERAL FORCE ESTIMATOR	
UNIVERSITY of SOUTHAMPTON	
DEPARTMENT of SHIP SCIENCE	
Title	
Size	Document Number
A	C60 R21-1-1
Date: September 10, 1992	Sheet of
REV	F

Fig. b3



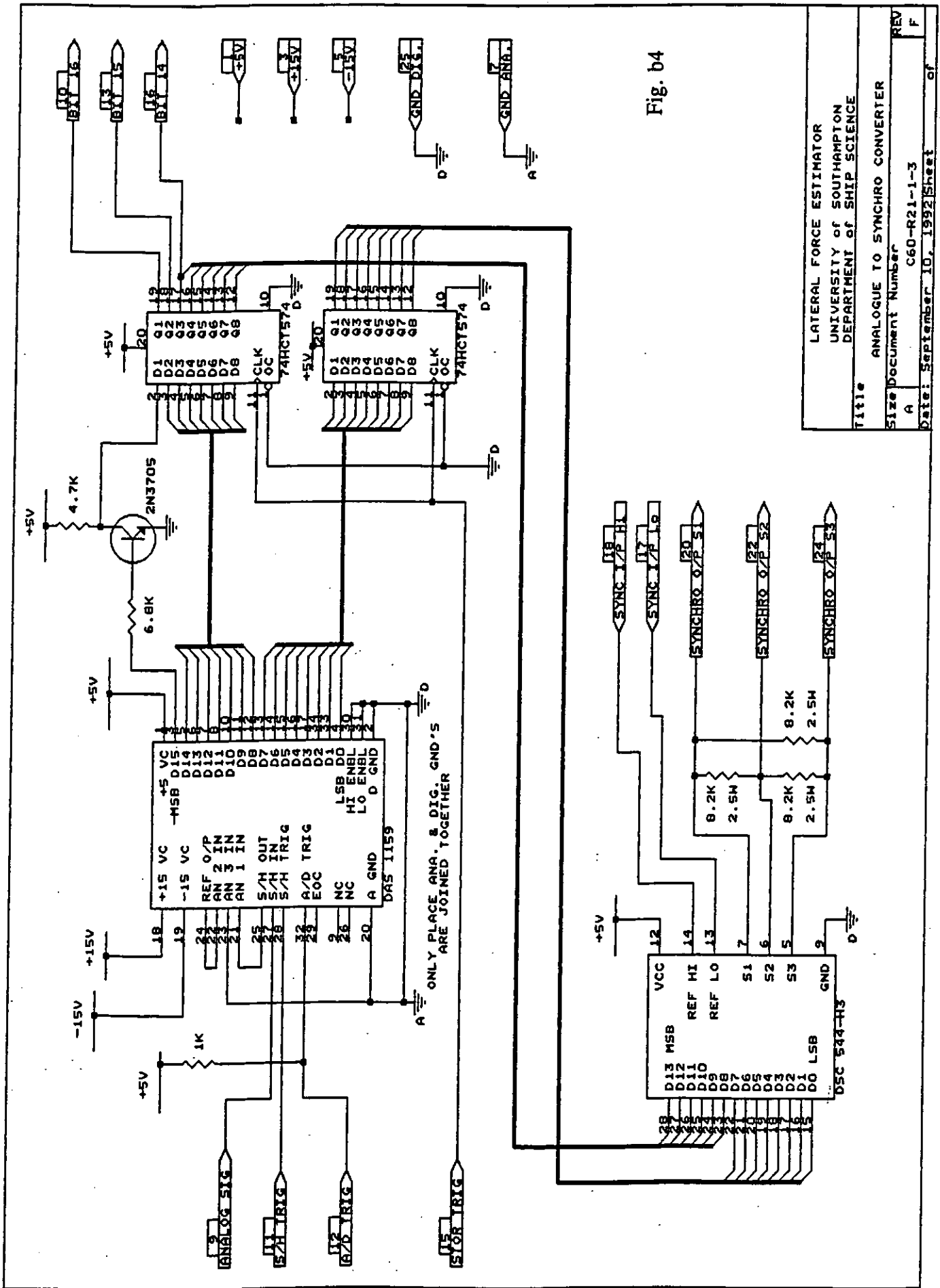
IC No	VCC	GND
U 1	16	8
U 2	14	7
U 3	14	7
U 4	16	8
U 5	5	10
U 6	16	8
U 7	14	7
U 8	14	7

LATERAL FORCE ESTIMATOR
UNIVERSITY OF SOUTHAMPTON
DEPARTMENT OF SHIP SCIENCE

Size Document Number
A C60-R21-1-2

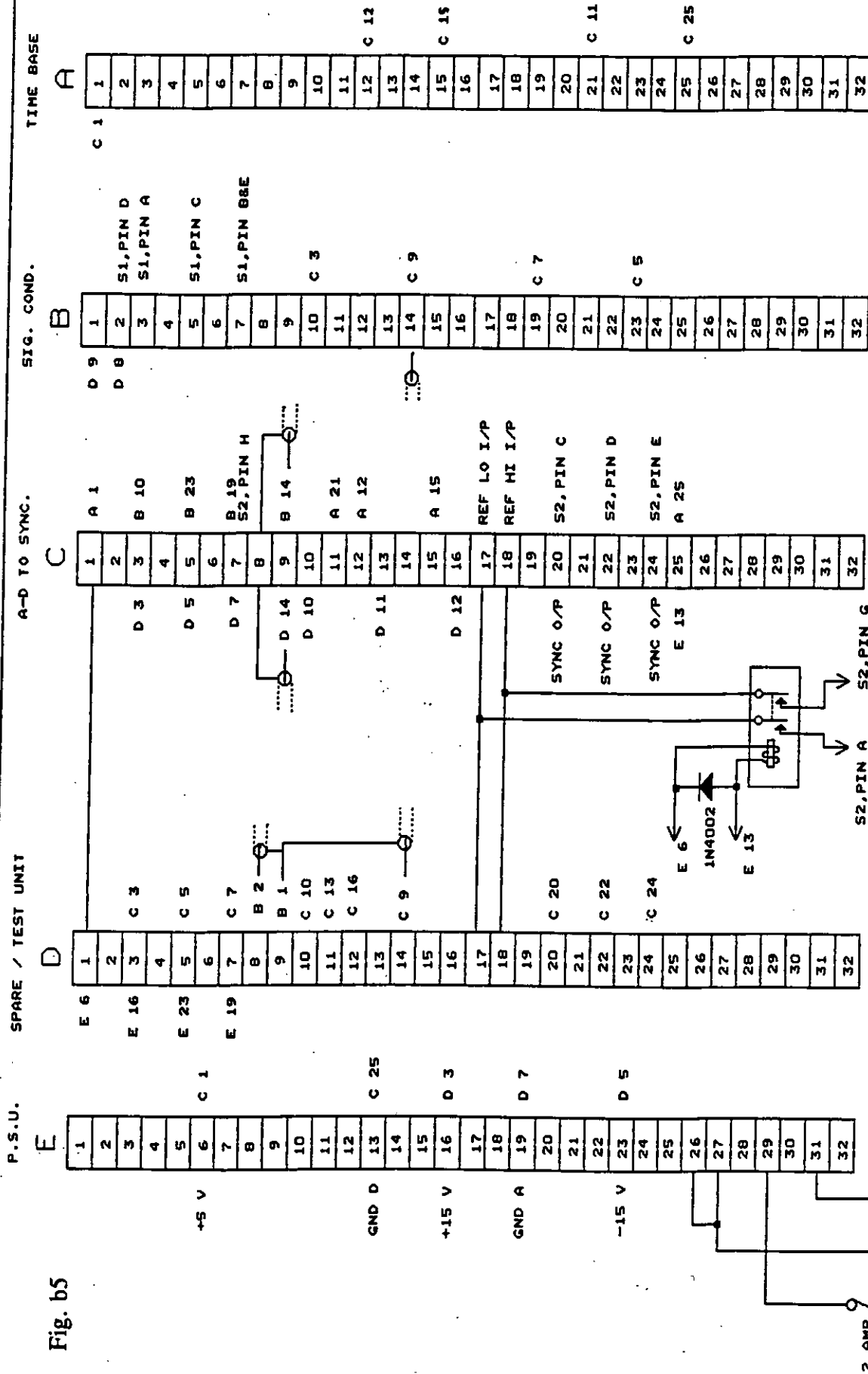
Date: September 10, 1992 Sheet
REV F

of



LATERAL FORCE ESTIMATOR		
UNIVERSITY OF SOUTHAMPTON		
DEPARTMENT OF SHIP SCIENCE		
Title		
ANALOGUE TO SYNCHRO CONVERTER		
Size Document Number		
A	C60-R21-1-3	REV F
Date: September 10, 1992 Sheet of		

Fig. b5



VIEW FROM REAR

LATERAL FORCE ESTIMATOR
UNIVERSITY OF SOUTHAMPTON
DEPARTMENT OF SHIP SCIENCE

rack wiring diagram

Document Number

C60-R21-1-5

Date: September 10, 1992

Sheet 1 of 1

REV

A

F

U.K. PATTERN
105 PLUG

+V SUPPLY (+15V) A
-V SUPPLY (-15V) C
OV SUPPLY B&E
SIGNAL D
CHASSIS GND F

RED A
BLUE C
GREEN B&E
YELLOW D
SCREEN N/C

AMPHENOL SOCKET
62GB-16J10-065N (639)
9002

+V SUPPLY
-V SUPPLY
OV SUPPLY
SIGNAL
N/C

COOLER/EXTRACTOR

U.K. PATTERN
105 SOCKET

SYNC O/P 1 C
SYNC O/P 2 D
OV SUPPLY H
SYNC O/P 3 E
SHIPS REF LO A
SHIPS REF HI G
SPARE B
SPARE F
N/C

RED
BLUE
GREEN
YELLOW
WHITE
BLACK
BROWN
VIOLET
SCREEN
N/C

AMPHENOL PLUG 608-56T-12-10-PE

PLB PIN B

PLB PIN C

NC

PLB PIN D

PLB PIN A

PLB pin J

NC

NC

SHIPS COMPUTER

Fig. b6

LATERAL FORCE ESTIMATOR
UNIVERSITY OF SOUTHAMPTON
DEPARTMENT OF SHIP SCIENCE

Title

Size Document Number

A

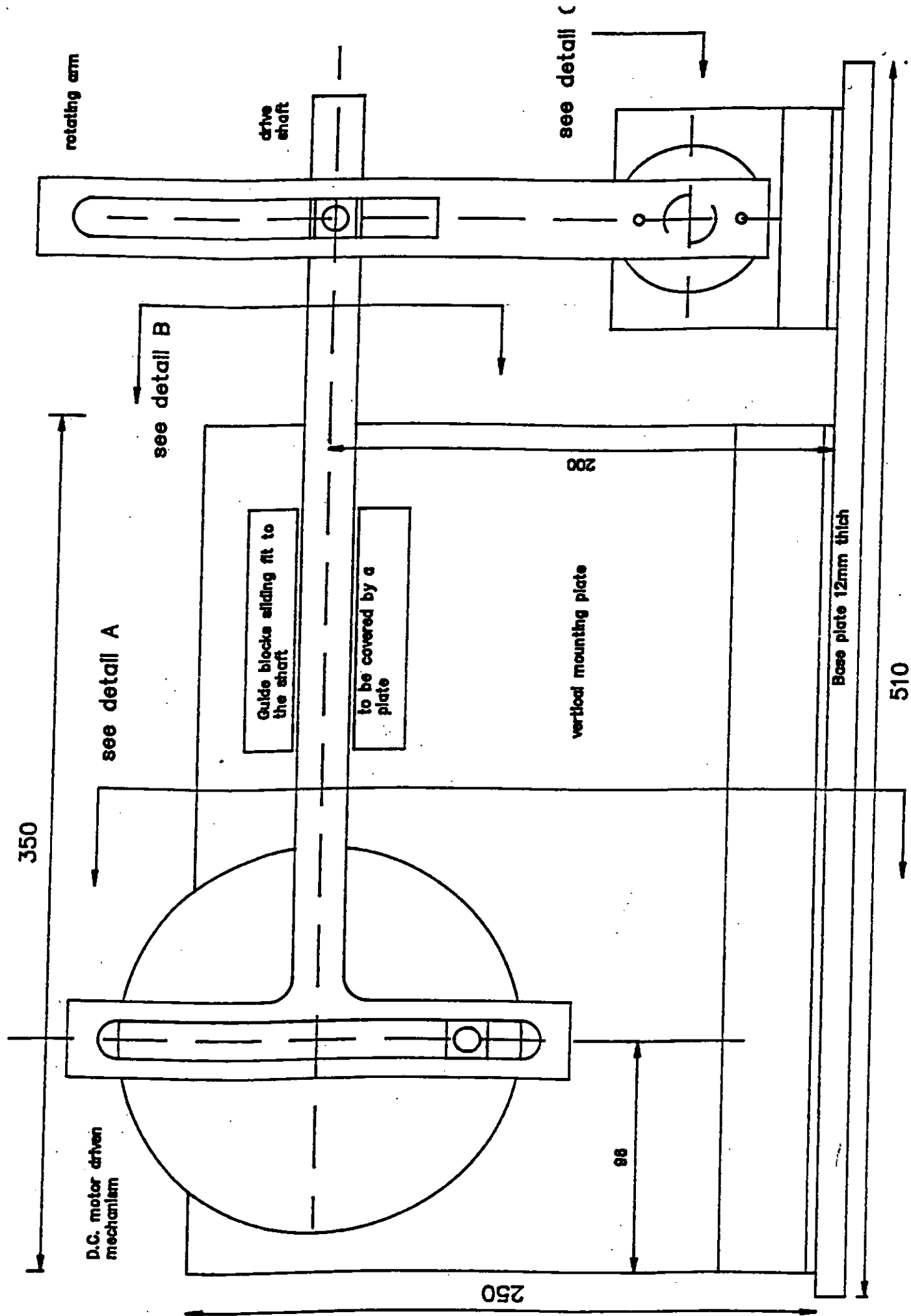
C60-R21-1-9

Date: September 10, 1992 Sheet

CABLE WIRING

REV

F



signal generator for the
active fin system
scale 2 : 1

Fig. c1

Fig. c2

DEPARTMENT OF SHIP SCIENCE
UNIVERSITY OF SOUTHAMPTON

ROLL OSCILLATOR MOTOR SPEED CONTROL
Size Document Number C60-R211-2-2
A

PROPOSED CIRCUIT

Fig. c2

DEPARTMENT OF SHIP SCIENCE
UNIVERSITY OF SOUTHAMPTON

ROLL OSCILLATOR MOTOR SPEED CONTROL

Size Document Number C60-R211-2-2

PROPOSED CIRCUIT

Fig. c2

DEPARTMENT OF SHIP SCIENCE
UNIVERSITY OF SOUTHAMPTON

ROLL OSCILLATOR MOTOR SPEED CONTROL
Size Document Number C60-R211-2-2
A

PROPOSED CIRCUIT

Fig. c2

DEPARTMENT OF SHIP SCIENCE
UNIVERSITY OF SOUTHAMPTON

ROLL OSCILLATOR MOTOR SPEED CONTROL
Size Document Number C60-R211-2-2
A

PROPOSED CIRCUIT

Fig. c2

DEPARTMENT OF SHIP SCIENCE
UNIVERSITY OF SOUTHAMPTON

ROLL OSCILLATOR MOTOR SPEED CONTROL
Size Document Number C60-R211-2-2
A

PROPOSED CIRCUIT

Fig. c2

DEPARTMENT OF SHIP SCIENCE
UNIVERSITY OF SOUTHAMPTON

ROLL OSCILLATOR MOTOR SPEED CONTROL
Size Document Number C60-R211-2-2
A

PROPOSED CIRCUIT

Fig. c2

DEPARTMENT OF SHIP SCIENCE
UNIVERSITY OF SOUTHAMPTON

ROLL OSCILLATOR MOTOR SPEED CONTROL
Size Document Number C60-R211-2-2
A

PROPOSED CIRCUIT

[illegible]

DEPARTMENT OF SHIP SCIENCE	
UNIVERSITY of SOUTHAMPTON	
Title	
ROLL OSCILLATOR PERIOD DISPLAY	
Size	Document Number
A	C60-R211-2-1
Date:	September 11, 1992
	Sheet of
	REV

DEPARTMENT of SHIP SCIENCE
UNIVERSITY of SOUTHAMPTON

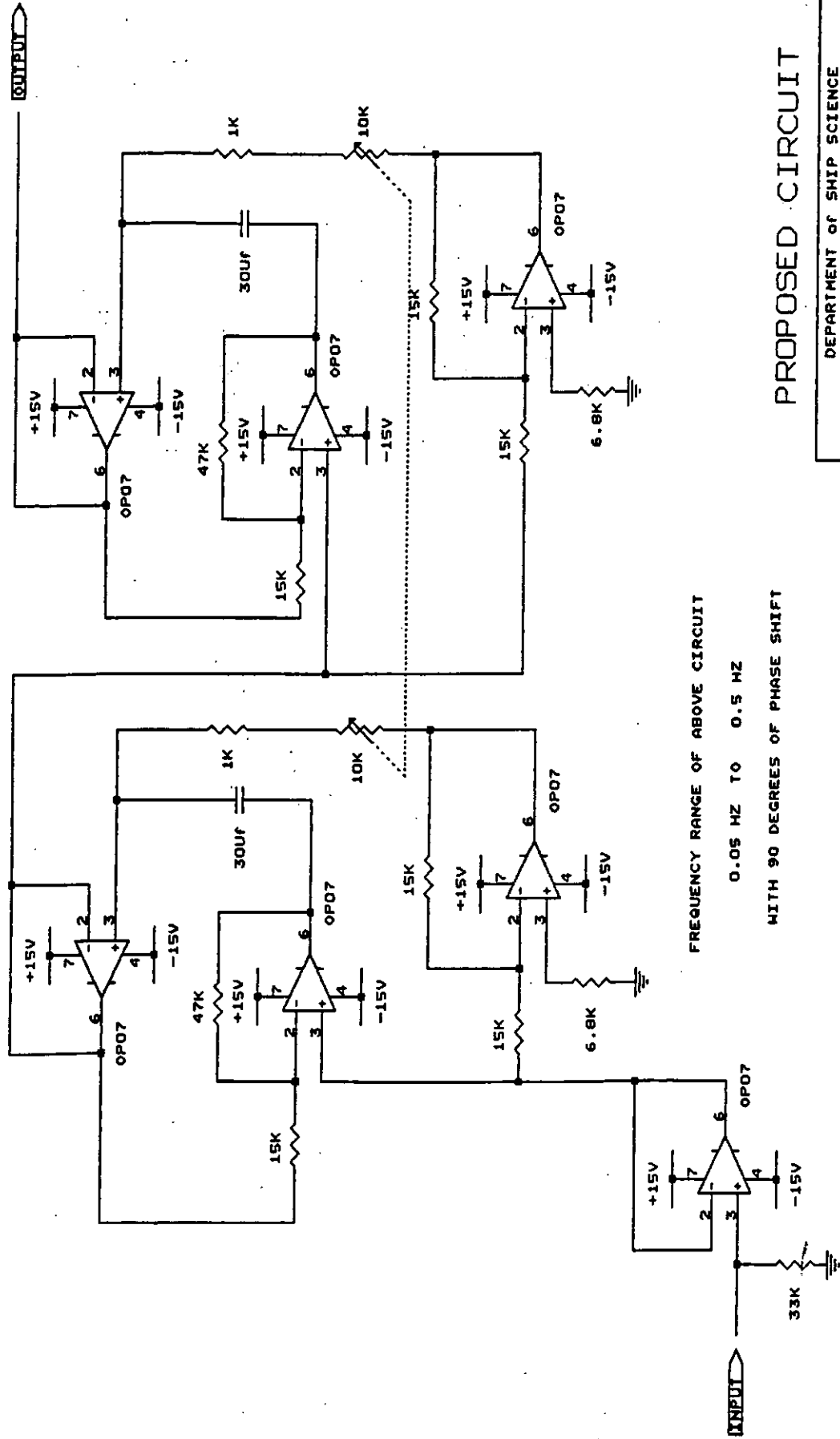
ROLL OSCILLATOR PERIOD DISPLAY

REV

1

30

Fig. c4



FREQUENCY RANGE OF ABOVE CIRCUIT
0.05 HZ TO 0.5 HZ
WITH 90 DEGREES OF PHASE SHIFT

PROPOSED CIRCUIT

DEPARTMENT OF SHIP SCIENCE	
UNIVERSITY OF SOUTHAMPTON	
Title	
90 DEGREE PHASE SHIFTER	
Size Document Number	
A	C60-R211-2-3
Date: September 11, 1992	
Sheet 1 of 1	